THE ENDOGENOUS RESPONSES OF THE MOUSE BRAIN TO AN ET-1 MEDIATED SMALL FOCAL ISCHEMIC INJURY

by

© Robert Francis Bartlett

A Thesis submitted to the

School of Graduate Studies

In partial fulfilment of the requirements for the degree of

Masters of Science in Medicine (Neuroscience)

Department of Biomedical Sciences/Faculty of Medicine

Memorial University of Newfoundland

October 2015

St. John's Newfoundland and Labrador

Abstract

Stroke is a debilitating disease that currently affects 50000 people in Canada yearly. Understanding the responses of the brain to a small clinically relevant model of ischemic stroke can lead to new and improved therapies to help improve stroke recovery. This thesis has characterized the endogenous responses to an Endothelin-1 (ET-1) mediated small focal ischemic injury over the first 10 days post-stroke. Major findings include the discovery and characterization of the spread of astrocyte activation across the cortex including activation in the contralateral cortex. Studies into the proliferative response of neural precursor cells showed a significant increase in the newborn neuroblast population.These results can lead to a greater understanding of the role of glial cells post-stroke and to the identification of an optimal time window in which to promote NPC survival post-stroke and improve stroke recovery.

Acknowledgements

I would like to thank my supervisor, Dr. Jackie Vanderluit, for all her help and guidance which allowed me to explore many opportunities throughout my program.

I would also like to thank the members of my supervisory committee, Dr. Michiru Hirasawa and Dr. Karen Mearow, who always provided insightful feedback that allowed me to improve my work.

I would like to acknowledge the support from the past and current members of the Vanderluit lab, who have helped me technically and through camaraderie during this program.

Finally, I would like to thank my family for their continuous support.

Table of Contents

List of Tables

List of Figures

List of Abbreviations and Symbols

Analysis of Variance – ANOVA

Anterior/Posterior – A/P

Blood brain barrier – BBB

Brain-derived neurotrophic factor – BDNF

Bromodeoxyuridine – BrdU

Degrees Celsius - ^{o}C

Doublecortin – Dcx

Endothelin 1 – ET-1

Epidermal growth factor – EGF

Fibroblast growth factor 2 – FGF2

Glial cell line-derived neurotrophic factor – GDNF

Glial fibrillary acidic protein – GFAP

Heat shock proteins – Hsps

Hour – hr

Immunohistochemistry – IHC

Insulin-like growth factor 1 – IGF-1

Liter – L

Medial/Lateral – M/L

Middle cerebral artery – MCA

Middle cerebral artery occlusion – MCAo

Molar – M

Nerve growth factor – NGF

Neural precursor cells – NPCs

Normal – N

Paraformaldehyde – PFA

Phosphate buffered saline – PBS

Pituitary adenylate cyclase-activating polypeptide – PACAP

Reactive oxygen species – ROS

Standard error of the mean – SEM

Subventricular zone – SVZ

Tissue plasminogen activator – t-PA

Vascular endothelial growth factor – VEGF

1 Introduction

1.1 Current state of stroke care and stroke recovery

Stroke is a far reaching disease, as part of vascular disease it is the most severely debilitating illness in the world. Vascular disease comprises 50,000 strokes in Canada annually (Adamson, Beswick, & Ebrahim, 2004; Hodgson, 1998). The majority of strokes are not fatal but disabling, with over 59% of people surviving the first year post-stroke (Bronnum-Hansen, Davidsen, & Thorvaldsen, 2001). Although many people survive their first stroke, the risk for subsequent strokes is high and there is a high rate of mortality within the first five years post-stroke (Bronnum-Hansen et al., 2001; Ng, Stein, Ning, & Black-Schaffer, 2007). Therefore, chronic care and recovery from stroke must be a key goal in alleviating the burden of vascular disease and the risk of subsequent strokes.

There are two types of stroke: ischemic and hemorrhagic. Ischemic stroke is responsible for 85% of all strokes and is defined as a lack of perfusion of blood to the brain (Smith, 2011). Hemorrhagic stroke is defined by the breakage of a blood vessel in the brain leading to intracranial bleeding, forming a hematoma. Patients who have an ischemic stroke have a better prognosis than those who suffer a hemorrhagic stroke (Andersen, Olsen, Dehlendorff, & Kammersgaard, 2009). This can be observed by comparing the 30-day mortality of ischemic stroke which is 12.7% compared to the 39.3% mortality for hemorrhagic stroke patients (Fang, Perraillon, Ghosh, Cutler, & Rosen, 2014). This thesis

focuses on ischemic stroke because of its higher prevalence and relatively higher survivability compared to hemorrhagic stroke.

The current state of stroke care is focused on reperfusion of the ischemic brain, followed by physical rehabilitation to aid functional recovery through the remapping of interrupted or lost motor pathways (Adkins-Muir & Jones, 2003; Fonarow et al., 2014; Kwakkel, 2006). Acute stroke care is focused on breaking the clot and establishing reperfusion to the injured area of the brain. To aid in breaking up the clot there is one drug treatment that can be applied acutely: tissue plasminogen activator (t-PA) (Banerjee, Williamson, Habib, & Chataway, 2012; Fisher et al., 2009). The major limitation of t-PA is that it must be given within a strict 4.5 hour time window post-stroke to have a positive effect on the patient's outcome (Del Zoppo, Saver, Jauch, & Adams, 2009; Hinkle & Guanci, 2007; Picanço et al., 2014). Unfortunately, many patients arrive to the hospital after this 4.5 hour window and have few treatment options available (Barber, Zhang, Demchuk, Hill, & Buchan, 2001). To address this need, over 100 clinical trials have been conducted to test novel neuroprotective therapies to improve post-stroke recovery. None have proven to be successful (Gladstone, Black, & Hakim, 2002). Improvement in novel neuroprotective therapies for stroke recovery is needed because of the high survival rate of patients with stroke and the risk of recurrent strokes (Roger et al., 2011; Zeiler et al., 2013). To improve post-stroke recovery, a new method must be exploited to lead to truly translational and successful therapies.

1.2 Pathology of ischemic stroke

Stroke is a disease with many different facets and a wide variability of outcomes. However, stroke follows a well-defined pathology (Brouns & De Deyn, 2009; Garcia et al., 1993). Ischemic stroke may begin as a quick event with the formation of a blood clot in the brain but the long term progression that follows, including paralysis and memory deficits continues for life (Garcia et al., 1993). While the physiological and functional responses to ischemic stroke have been studied, there is still a lack of understanding of the cellular response including the neural precursor response, and the glial response to a small focal ischemic injury (Deb, Sharma, & Hassan, 2010; Dereski, Chopp, Knight, Rodolosi, & Garcia, 1993; Hall, Davies, Stamp, Clamp, & Bigley, 2013; Neher et al., 2013). In addition, co-morbidities such as dementia, diabetes, atrial fibrillation and coronary artery disease have an impact on stroke and outcomes post stroke (Fischer et al., 2006). Ischemic injuries are variable depending on the size, location and the collaterals in the brain, but many injuries have similar pathology and common pathways.

Ischemic stroke has a large number of causes ranging from small vessel disease to large artery occlusion. A large proportion of strokes arise from clots within the branches of the middle cerebral artery (MCA) (Carmichael, 2005). Occlusion of these blood vessels restricts the nutrients available to the surrounding tissue. This lack of oxygen and glucose to the brain rapidly causes cell death (Deb et al., 2010). There is a combination of both necrotic and apoptotic cell death post-stroke (Hall et al., 2013). Cell death within the core of the infarct is primarily necrotic because the dying cells do not have the required energy to activate the apoptotic cascade (Deb et al., 2010). Cell death causes cells to burst and

release intracellular contents into the extracellular space. These contents include glutamate and reactive oxygen species (ROS) that are toxic and cause apoptosis to the surrounding cells (Deb et al., 2010). Secondary cell death surrounding the infarct transitions into a mixture of apoptotic and necrotic cell death over the following days post-stroke.

The area surrounding the infarcted core is an area of tissue known as the penumbra that, while hypo-perfused, can contain viable tissue (Astrup, Siesjo, & Symon, 1981; Baron, Yamauchi, Fujioka, & Endres, 2014; Deb et al., 2010). This area is a well-known hallmark of stroke pathology (Garcia et al., 1993). Although the penumbra is at risk of further cell loss, the viable tissue there has the potential to be saved if action is taken quickly to resolve the stroke (Albers et al., 2006; Baron et al., 2014). The penumbra is a crucial area post-stroke that if saved can drastically change the outcome of post-stroke recovery.

A major part of the post-stroke response from glial cells is to create a barrier that separates the healthy and injured tissue. This barrier, often seen years post-stroke in human patients, is called the glial scar (Rolls, Shechter, & Schwartz, 2009). The scar is composed primarily of activated astrocytes as well as some immune cells, together they form a physical barrier surrounding the ischemic core (Huang et al., 2014; Stoll, 1998; Yuan & He, 2013). The formation of the glial scar separates the ischemic core from the healthy brain, and is seen in all ischemic injuries (Stichel & Müller, 1998). The glial scar prevents excitotoxicity and further apoptosis of cells in the cortex, by limiting the spread of glutamate and ROS within the ischemic core (Brouns & De Deyn, 2009). The

formation of the glial scar is a robust response that occurs within the first hours to days post-stroke (Rolls et al., 2009). The formation of the glial scar plays an important aspect in post-stroke pathology, by defining the size of the infarct.

The vasculature in the post-ischemic brain is seen as one area where intervention can improve stroke recovery. Vascular disease can increase the breakdown of the blood brain barrier (BBB), resulting in immune cells infiltrating the ischemic region (Bush et al., 1999; Stoll, 1998; Tennant & Brown, 2013). Unfortunately, these cells not only clear the dead and dying cells within the core, but also destroy some of the viable brain tissue surrounding the core (Neher et al., 2013). The vascular response to stroke is of the utmost importance to aiding in stroke recovery (Schellinger et al., 2013). The vascular response is comprised of the reperfusion, which provides oxygen and glucose to the injured area but also the creation of new blood vessels. The vasculature delivers nutrients once reperfusion is established and is used as a scaffold for neuroblasts post-stroke (Brouns & De Deyn, 2009; Kahle & Bix, 2013; Thored et al., 2006). This is reinforced by the fact that a lack of viable blood vessels limits neuroblast migration to the site of injury in the post-ischemic cortex (Kahle & Bix, 2013). Blood vessels act as both a structural support and a nutrient delivery system to the brain. Breakdown of blood vessels leads to cell death due to a lack of nutrition and oxygen to the surviving tissue.

Ischemic stroke is a diverse disease with many players. Firstly, there is necrotic cell death associated with a lack of blood flow to the ischemic region. This is followed by an increase in apoptotic cell death and a glial cell response, as the intracellular components of necrotic cells from the ischemic core are released. With the breakdown of blood

vessels within the ischemic region, the brain also loses a method in which to transport oxygen and nutrition to surviving cells and a structural support. Together these responses interact and form the pathology of an ischemic injury.

1.3 The pro-survival and regenerative responses to ischemic stroke

While there is an increase in cell death and glial cell activation as part of the endogenous response to ischemia, there is also a pro-survival response. This can be seen by the specific increase in pro-survival and growth factors in the post-ischemic cortex, such as brain-derived neurotrophic factor (BDNF) which has been implicated in improved recovery and angiogenesis (Lopez-Lopez, LeRoith, & Torres-Aleman, 2004; Ploughman et al., 2007). Taking advantage of the endogenous pro-survival response allows for new treatments to improve stroke recovery.

To improve stroke recovery, a window for introduction of novel therapies has been suggested. A window of 5 to 14 days post-stroke has been suggested to yield optimal recovery (Krakauer, Carmichael, Corbett, & Wittenberg, 2012; MacLellan et al., 2011; Murphy & Corbett, 2009). A number of studies have focused on identifying the optimum time point following stroke to begin physical rehabilitation in order to maximize functional recovery. Studies that started physical rehabilitation between 5 to 14 days post-stroke found animals had improved functional recovery. Functional recovery was not observed when physical rehabilitation was started at 30 days (Biernaskie, Chernenko, & Corbett, 2004). This is reinforced through clinical studies where earlier rehabilitation resulted in better functional outcomes in humans (Horn et al., 2005). One of the potential reasons why early intervention leads to improved functional outcomes is that higher

levels of growth factors are present at the early time points. Growth factors that have been implicated in axonal sprouting, such as GAP 43, CAP 23 and c-JUN are upregulated by 3 days post-stroke and remain elevated until 28 days post-stroke (Carmichael et al., 2005). This is followed by the upregulation of axonal growth inhibitors, such as Aggrecan, and NG2. The majority of these inhibitory genes have peak levels of gene expression from 14 to 28 days post-stroke (Carmichael et al., 2005). This period, when growth factors are at high levels and before growth inhibitors are upregulated has been termed a critical period to improve stroke recovery (MacLellan et al., 2011). A potential time window for optimal rehabilitation can be found by overlapping the periods of effective rehabilitation with the upregulation of survival genes but excluding the period of increased inhibitory genes (Fig. 1.1). This period was defined to help improve rehabilitation and increase remapping of motor-maps (Harrison & Murphy, 2012). Molecular approaches can help improve rehabilitation since the basis for the period is defined by the changes of growth and inhibitory molecular markers (Murphy & Corbett, 2009). Therefore, it appears that a larger pro-survival and growth factor response during the critical period is necessary to have a meaningful impact on stroke recovery (Osman, Porritt, Nilsson, & Kuhn, 2011; Parent, Vexler, Gong, Derugin, & Ferriero, 2002). Unfortunately, there is not a large endogenous neurogenic response post-stroke. Identification of novel targets that have significant impact on the post-ischemic cortex and enhance the endogenous neurogenic response can become an effective treatment alone or used in parallel with other treatments to create a synergistic effect.

Figure 1.1: Identification of an optimal time window to introduce therapy post-stroke.

Timeline showing time windows of growth genes (red) and inhibitory genes (blue) as well as the optimal time window to start physical rehabilitation post-stroke (green) (Carmichael et al., 2005; Harrison & Murphy, 2012).

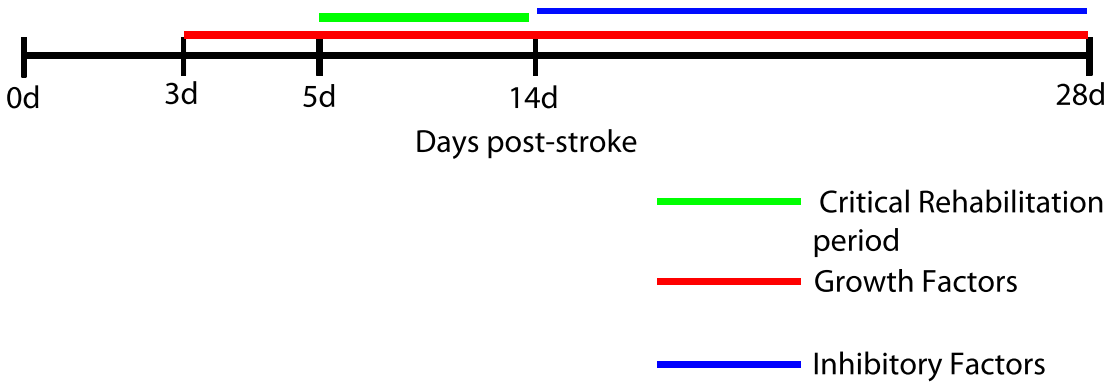
0d
3d
5d
14d
28d
Days post-stroke
Critical Rehabilitation period
Growth Factors
Inhibitory Factors

In response to an ischemic injury, the post-ischemic cortex forms a glial scar that limits the size of injury. In addition to a glial scar that controls the spread of the size of injury, there is a pro-survival response within the post-ischemic cortex. The pro-survival response consists of containing the damage and attempting to maintain the survival of neurons in the peri-infarct area. How the pro-survival response promotes stroke recovery has been well studied (Christie & Turnley, 2012; MacLellan et al., 2011). BDNF is an example of a growth factor that increases in the post-ischemic cortex. BDNF is a neurotrophic factor that improves functional recovery, and if BDNF is knocked down then functional recovery is delayed. BDNF has a critical threshold for its maximal pro-survival effect post-ischemic injury (MacLellan et al., 2011). To improve functional recovery, studies have used multiple therapies to assess if there is synergy between treatments. The use of multiple treatments, such as BDNF treatment and enriched physical rehabilitation appears to have a synergistic effect, leading to the term "enhanced rehabilitation" (Hicks, MacLellan, Chernenko, & Corbett, 2008). Further examples of growth factors can be found in Table 1.1.

Table 1.1 Response of growth factors post stroke

Factor	Expression post-stroke	Effect on NPCs	References
Epidermal growth factor (EGF)	Upregulated	Increases proliferation and migration of NPCs within the SVZ	(Teramoto, Qiu, Plumier, & Moskowitz, 2003)
BDNF	Highly upregulated	Differentiation and survival of NPCs within the SVZ	(Im et al., 2010)
Nerve growth factor (NGF)	Upregulated	Improves survival of NPCs within the SGZ	(Zhu et al., 2011)
Fibroblast growth factor 2 (FGF2)	Upregulated	Increases proliferation of NPCs within the SVZ	(Türeyen, Vemuganti, Bowen, Sailor, & Dempsey, 2005)
Glial cell line-derived neurotrophic factor (GDNF)	Upregulated	Increases proliferation of NPCs within the SVZ	(Arvidsson, Kokaia, Airaksinen, Saarma, & Lindvall, 2001; Kobayashi et al., 2006)
Insulin-like growth factor 1 (IGF-1)	Stable	Induce migration of NPCs within the SVZ	(Aberg, Aberg, Hedbäcker, Oscarsson, & Eriksson, 2000)
Pituitary adenylate cyclase-activating polypeptide (PACAP)	Upregulated	Survival of neurons and maintenance of the NPC population	(Chen et al., 2006; Ohta, Gregg, & Weiss, 2006)
Vascular endothelial growth factor (VEGF)	Stable	Proliferation and migration within the SVZ	(Wittko et al., 2009)

Unfortunately, out of all these factors only EGF, which maintains the proliferation of the NPC pool, and FGF2 which increases neurogenesis in the rostral migratory stream regulate NPCs *in vivo* (Christie & Turnley, 2012; Kuhn, Winkler, Kempermann, Thal, & Gage, 1997). However, these two factors have not been shown to improve stroke recovery in a clinical setting. While there are a number of pro-survival factors identified and tested, none have had a significant improvement on stroke recovery. To improve recovery, identification of an optimal time period of NPC activity post-stroke could provide a new time point where these pro-survival factors could have their greatest impact.

The pro-survival response to an ischemic injury has generated hope that the exogenous application of growth and pro-survival factors can lead to improved stroke recovery. Therefore, the development of an optimal time window where physical rehabilitation and molecular approaches have the greatest effect is crucial to maximize the potential impact of novel therapies post-stroke. Understanding the endogenous survival response allows for novel therapeutic targets to be identified and studied in greater detail. This can ultimately lead to the development of new therapies and improve stroke care.

1.4 Glial response to ischemic stroke

Most research focuses on the responses of the neuronal population to an ischemic injury. However, to provide a full picture of an ischemic injury, the glial population must also be investigated since it plays a role in injury. This allows researchers to understand how potential therapeutics will be affected by the astrocyte and microglial cell population (L. Huang et al., 2014; Stoll, 1998). The glial response to injury is robust and seen in all

central nervous system (CNS) injuries (L. Huang et al., 2014; Rolls et al., 2009; Stichel & Müller, 1998; Yuan & He, 2013). The major response of astrocytes and microglia after an ischemic injury is to form a physical barrier surrounding the injury to sequester the injury from spreading (L. Huang et al., 2014; Stoll, 1998; Yuan & He, 2013). The formation of this scar has a large effect on recovery, as it contains the dead and dying cells within the ischemic core to prevent the spread of ROS (Yuan & He, 2013). Furthermore, when the glial scar is prevented from forming there is a significant decrease in stroke recovery (Sofroniew, 2009). However, the glial scar could also become a barrier to neural repair in the brain and force remapping of connections to the surviving cortex (Benowitz & Carmichael, 2010). Therefore, the time of glial scar formation and characterization of the immune cell response may identify good targets for improving stroke recovery.

1.4.1 Astrocytes

Astrocytes are found in all parts of the brain and act to provide nutrition as well as support to neurons. Astrocytes are the main glial cell type found in the brain comprising 40-50% of all glial cells (Aldskogius & Kozlova, 1998). Following injury astrocytes become activated and become part of the response to the injury. Specifically, astrocytes will respond to the injury by upregulating glial fibrillary acidic protein (GFAP), a filamentous protein that is expressed in astrocytes and ependymal cells of the CNS. This thesis has taken advantage of this by examining the activation of astrocytes, which have increased numbers of processes and swollen processes along with increased GFAP staining (Aldskogius & Kozlova, 1998). The response of astrocytes to an ischemic stroke is highly regulated and follows a distinct pathological progression from the upregulation

of GFAP, changes in morphology and leading to their incorporation in the glial scar (Stichel & Müller, 1998; Stoll, 1998). In addition to the glial scar there are other effects of ischemic stroke on the glial population.

Following stroke, astrocytes proliferate creating more activated astrocytes within the injured brain (Walberer et al., 2010). These astrocytes upregulate a host of proteins to either communicate with other cells, such as connexins for the formation of gap junctions, or to aid in neuronal survival, such as neurotrophic factors and heat shock proteins (Hsps) (Aldskogius & Kozlova, 1998; Barreto, White, Xu, Palm, & Giffard, 2012). The roles of these activated astrocytes includes the uptake of excitotoxic glutamate and ROS (Takatsuru et al., 2013). Astrocytes are also able to exert both pro- and anti-inflammatory effects on the microglial immune response (Min, Yang, Kim, Jou, & Joe, 2006). Astrocytes are responsible for a large portion of the post-ischemic response, ranging from glial scar formation to supporting the surrounding cells. It still remains unknown when astrocytes become activated, and where the activation spreads in the ischemic cortex following a small focal ischemic injury. This thesis examines when GFAP is upregulated and the area of astrocyte activation following a focal ischemic injury.

1.4.2 Immune response

The immune system responds to changes to the body. This response also extends to ischemic injuries in the brain. Increased necrotic cell death and the release of intracellular contents activate a large immune response to ischemic injury (Becker, 1998; Benarroch, 2013). The immune response is led by microglia and macrophages that, when activated,

will upregulate the cell surface marker CD-68 (Benarroch, 2013). Microglia are the resident immune cells in the brain (Burns & Steinberg, 2011). If there is a breakdown in the BBB during the ischemic injury, macrophages from the blood stream will also respond to the injury (Bush et al., 1999). Activated immune cells can be identified with antibodies to the cell surface marker CD-68, however microglia and macrophages, while residing in two different parts of the body, are indistinguishable based on this immunohistochemical marker (Guillemin & Brew, 2004). Microglia and macrophages are able to regulate the clearing of the infarct site through phagocytosis of the dead and dying cells (Iadecola & Anrather, 2011). The glial scar forms a barrier separating the activated microglia and macrophages from the healthy tissue thereby delimiting the size of the injury.

Immune cells have a positive role within the injury, by clearing cellular debris, however immune cells also create a cytotoxic environment by secreting pro-inflammatory factors (Price et al., 2006). These pro-inflammatory factors can induce apoptotic cell death in neurons within and surrounding the infarct and in NPC migrating to the infarct (Thored et al., 2006). This cytotoxic environment is caused by activated immune cells, specifically, the M1 polarized macrophages and microglia (Benarroch, 2013). The polarization of immune cells as either phagocytic M1 or neurotrophic M2 is critical to understanding the role these cells play in the post-ischemic cortex (Taylor & Sansing, 2013). The M1 phagocytic immune cells are responsible for causing delayed cell death of neurons and glial cells surrounding the infarct up to 7 days post-stroke (Neher et al., 2013). Studies which depleted immune cells from the brain resulted in less brain atrophy (Neher et al.,

2013). This shows that immune cells significantly modulate the outcome of the post-ischemic brain. Knowing when immune cells first become activated, and when they switch from an M1 phagocytic state to an M2 neurotrophic state may help in the future to modulate the survival of NPC to have the greatest impact on stroke recovery.

1.4.3 Removing the glial response

The glial response has a large impact on the post-ischemic cortex. Studies which have removed or modified the glial response have improved our knowledge of the role glial cells play in the post-ischemic cortex. Many studies have focused on reducing or completely removing the glial scar as it was seen as a barrier to the endogenous neurogenic response (Sofroniew, 2009; Yuan & He, 2013). The glial scar forms a physical barrier that NPCs will migrate towards but are not able to penetrate. Thus a smaller or more porous glial scar may allow NPCs to penetrate the injury and help regenerate a portion of the lost tissue. One study knocked-out the glial scar-forming astrocytes. To mitigate the confounding effects of knocking out all astrocytes, a knock-out that provided both temporal and type-specific control was generated. This was achieved using GFAP-induced expression of herpes simplex virus thymidine kinase combined with the anti-viral drug, ganciclovir, which selectively killed the astrocyte population. However, when astrocyte numbers were reduced and no glial scar formed, a larger ischemic injury was observed compared to control animals (Sabelström et al., 2013). This evidence shows that astrocytes and the glial scar also have a protective role in the injured brain. Therefore, it is critical to learn more about the glial scar, when it forms, and how it plays a positive role in mitigating the size of an infarct by limiting expansion

of the injury site. Understanding the glial response can lead to new therapeutic targets for improving stroke recovery.

1.5 Stroke and Neural stem cells

The hope that neural stem cells can play a role in recovery from stroke has been investigated in earnest for the past two decades. This was accelerated when it was discovered that NPCs are able to respond to an ischemic injury and migrate to the site of injury (A. Arvidsson, Collin, Kirik, Kokaia, & Lindvall, 2002; Parent et al., 2002). The ability of NPCs to give rise to the three major cell types in the brain; neurons, astrocytes and oligodendrocytes, increases the hope that these cells can help aid in stroke recovery (Gage, Ray, & Fisher, 1995; Kornblum, 2007). The question remains: if NPCs migrate to the site of injury and can differentiate into mature cells, why is there no tissue regeneration or repair of the injury site and a lack of full functional recovery?

NPCs respond to an ischemic injury by proliferating and migrating to the site of injury, but these NPCs do not integrate into the post-ischemic cortex. The majority of these NPCs do not become mature neurons (Kokaia, Thored, Arvidsson, & Lindvall, 2006; Osman et al., 2011; Parent et al., 2002). Therefore the question remained what is the fate of these NPCs? To assess if neuroblasts, a subtype of NPCs, which migrate to the site of injury play a role in stroke recovery, a knock-out model for neuroblasts was produced. Doublecortin (Dcx) positive neuroblasts were selectively knocked out by transfection of herpes simplex virus thymidine kinase and thereby, became sensitive to the anti-viral drug ganciclovir. Knocking out neuroblasts caused an increase in the infarct size and significantly greater sensorimotor deficits post-stroke (Jin, Wang, Xie, Mao, &

Greenberg, 2010). This demonstrated that neuroblasts have a role in promoting stroke recovery, although they do not become mature neurons. NPCs have the ability to provide trophic support through the secretion of growth and survival factors to the surrounding cells (MacLellan et al., 2011; Tsai et al., 2006). Therefore, by remaining in an undifferentiated state, neuroblasts may provide trophic factor support to cells surrounding the infarct (Tsai et al., 2006). Further studies exploring when NPCs respond to ischemic injuries and how they minimize the size of injury may potentially identify novel treatments post-stroke.

Unfortunately, the majority of NPCs and specifically neuroblasts do not survive upon migrating to the infarct. These neuroblasts die through apoptosis (Thored et al., 2006). Blocking apoptosis has been shown to increase their numbers in the post-ischemic cortex (Osman et al., 2011). If apoptosis can be specifically inhibited within neuroblasts, then identifying their role in the post-ischemic cortex and methods to promote their neural differentiation may be found. One method to improve the survival of NPCs post-stroke is overexpressing the anti-apoptotic protein, Bcl-xL which blocks apoptotic cell death (Doeppner et al., 2010). Improving NPC survival may allow differentiation into mature cell types in the post-ischemic cortex and/or the survival of the surrounding cells through trophic support. Improving the survival of NPCs in the post-ischemic cortex and specifically blocking apoptosis in NPCs may lead to a viable therapy post-stroke.

Minimizing the size of ischemic injuries and how neuroblasts respond to an ischemic injury are currently being studied. Previous studies on the time course of the neuroblast response and migration towards the site of injury have been confined to a resolution of

weeks (A. Arvidsson et al., 2002; Parent et al., 2002). As part of the NPC response post-stroke, an increase in migratory neuroblasts in the ischemic cortex peaked by 1 week post-stroke and continued to be elevated up to 16 weeks post-stroke (Kokaia et al., 2006). To characterize the acute phase post-stroke, this study examined the cellular response to stroke over the first 10 days when the NPC response is at its peak. This examination may potentially lead to identifying an optimal time point of the NPC response that can then be exploited for interventional therapies.

The response of NPCs and the hope to improve functional recovery post-stroke has been studied in earnest over the past decades with many different approaches being used to understand and exploit NPCs. This has led to many different avenues into using NPCs post-stroke including increasing endogenous precursor survival and exogenous implantation of hydrogels with NPCs (Lagace, 2012). Unfortunately, there remains a need to uncover the optimal time window post-stroke where there is a peak response from the neural precursor population.

1.6 Models of ischemic stroke in rodents

To understand ischemic stroke and to test novel therapies there must be clinically relevant laboratory models of ischemic stroke. Animal models of stroke, especially rodent models, have become the standard in testing novel therapies for stroke recovery. Each model of stroke has its own specific strengths and weaknesses and no model, however well-planned, will be able to perfectly mimic human stroke (Carmichael, 2005). Therefore each model will have specific advantages and disadvantages.

1.6.1 Criteria

All models need to have the hallmarks of the disease they are modeling; therefore there are universal criteria that must be addressed for clinical validity. The majority of rodent stroke models use rats, but more studies are adapting rat models for use with mice to take advantage of transgenic strains (Clarkson et al., 2013; Horie et al., 2008; Osman et al., 2011; Roome et al., 2014; Tennant & Brown, 2013). A number of characteristics of human stroke that should be modeled in experimental stroke models include: the size of ischemic injuries and reperfusion of the brain after stroke. The first characteristic is the size of the stroke. When the injury comprises over 145 cm^3 in size, or over 30% of cortex it is defined as a malignant stroke in humans (Carmichael, 2005; Wartenberg, 2012). These strokes are extremely debilitating and are associated with low survival and poor stroke recovery. While it would be ground-breaking to be able to reverse the low survival of these larger strokes, currently the greatest gains can be made by treating and improving the recovery of smaller strokes. Therefore, the goal is to model smaller strokes in which outcomes are more favourable and have the greatest potential to be responsive to novel therapies. The second characteristic is reperfusion following ischemic stroke. Spontaneous reperfusion occurs in 20% of ischemic strokes (Olsen & Lassen, 1984). The introduction of clot busting agents are increasing the rate of reperfusion (Carmichael, 2005). Stroke models that allow for reperfusion are needed to model the current state of stroke. In this study, a small focal stroke in which reperfusion occurs was used.

1.6.2 Endothelin-1 induced ischemia

A focal model of ischemia and the one that will be used in this thesis is intracortical injections of Endothelin-1 (ET-1). ET-1 is a vasoactive peptide and when injected intracortically will lead to a lack of blood flow due to constriction of the blood vessels surrounding the injection site (Adkins-Muir & Jones, 2003; Fuxe et al., 1997; Hughes et al., 2003). After the injection, ET-1 is metabolized and reperfusion is established (Macrae, Robinson, Graham, Reid, & McCulloch, 1993). ET-1 acts on two receptors in endothelial cells lining the blood vessels: endothelin receptor A and endothelin receptor B. Endothelin receptor A has a vasoconstrictive effect on endothelial cells and endothelin receptor B has a vasodilative response (Horie et al., 2008). One challenge for using ET-1 as a model of focal ischemia in mice is that expression of the vasodilative endothelin receptor B is twice as high as the vasoconstrictive endothelin receptor A (Wiley & Davenport, 2004). This receptor profile is different from that of rats, leading mice to be less sensitive to ET-1 induced ischemic injury. However, Dr. Vanderluit's lab has recently developed a model of ischemic injury in the mouse using multiple intra-cortical injections of high concentrations of ET-1 to create a reproducible infarct in the mouse forelimb motor cortex (Roome et al., 2014). With the new model of ET-1 injections, there are more opportunities to use ET-1 as a model of ischemic stroke in mice.

The use of ET-1 injections as a model of ischemic stroke has grown in popularity in rats because of its ability to create localized infarcts (Carmichael, 2005). An advantage of the ET-1 injection model is that is it possible to target infarcts to a specific location to cause either a mostly gray matter injury such as in this study or an injury targeting the white

matter. The MCAo model causes extensive damage to both gray and white matter and is not useful for studying the impact of infarcts that are localized to the gray matter. This is important for translation studies where gray matter injuries have been shown to be at a higher risk of permanent damage in human strokes. Stroke models that exclusively target the gray matter therefore are important to understanding these injuries (Falcao et al., 2004). Infarcts caused by ET-1 injections into rodents are well defined and reproducible based upon a strong correlation between ET-1 dosage and infarct volume(Fuxe et al., 1997). ET-1 injuryies show evidence of infarction in the area surrounding the ET-1 injection site where damage has been confirmed using cresyl violet and fluoro Jade-B staining (Macrae et al., 1993; Tsenov, Mátéffyová, Mareš, Otáhal, & Kubová, 2007). As modern techniques become available and refined, more aspects of human stroke in rodents are able to be accurately modeled. Although no model of ischemic stroke will ever be able to truly mimic human stroke the use of *in vivo* models is crucial to the improvement of stroke recovery.

1.7 Rationale

Despite numerous studies focused on endogenous NPCs post-stroke, there is a lack of successful therapies arising from these studies (Gladstone et al., 2002). One of the major hurdles in harnessing the neurogenic abilities of NPCs is that the vast majority of NPCs undergo apoptosis and die prior to contributing to the recovery post-stroke (A. Arvidsson et al., 2002; Osman et al., 2011). However, new studies have shown that some cells are able to survive and mature into functional interneurons in the striatum (Hou et al., 2008). This leads to the promise that NPCs may be able to improve stroke. To optimize the use

of NPCs as a therapy, there must be improved survival of NPCs post-stroke. To increase the survival of NPCs, identifying the optimal time window in which to manipulate the largest number of NPCs needs to be identified to have the greatest possible impact on recovery post-stroke. Additionally, glial cells can play a role in supporting NPCs post-stroke and control the size of the infarct (Sabelström et al., 2013). Therefore this thesis focuses on assessing and characterizing the glial response to stroke. This is in addition to analyzing the proliferation of NPCs following a small focal ischemic injury. Understanding when glial cells and NPCs respond to a focal ischemic injury can help identify the optimal window to improve NPC survival post-stroke.

1.7.1 Research Goal:

The characterization of a small ischemic injury and the responses of glia and NPCs in the hope of identifying an optimum time period for interventional therapies.

1.7.2 Aims:

To address the research goal this thesis has two aims:

1. Characterize infarct progression and the glial response following a small focal ischemic injury.
2. Characterize the response of NPCs, specifically newly born neuroblasts over the first 10 days post-ischemic injury.

2 Methods and Materials:

2.1 Mice

Adult male FVBN mice were singly housed on a 12hr light/dark cycle. Mice had access to water and standard rodent chow *ad libitum*. All experiments were approved by the Memorial University institutional animal care committee in accordance with the guidelines from the Canadian Council on Animal Care.

2.2 Surgery

2.2.1 Endothelin-1 surgery

Mice were anesthetized using isoflurane (Aerrane, 02225875, Baxter, Ontario, Canada) and placed into the stereotaxic instrument (308019R, David Kopf Instruments, California, United States). Mice were kept warm with a heating pad throughout the surgery. Lanalin was placed on the eyes to prevent drying. 50μL of buprenorphine was injected into the rump. The fur covering the top of the skull was removed using a razor. An incision was made in the scalp in an anterior to posterior direction allowing access to the skull. The periosteum was scraped away using a cotton tipped applicator. Lambda and Bregma sutures were marked using an ultra fine tipped marker. Injection co-ordinates were marked onto the skull. An Ideal Microdrill (67-1000, Cellpoint Scientific, Maryland, United States) was used to drill into the skull. The meninges were then scraped away allowing access to the cortex. Either Endothelin-1 or 0.9% NaCl solution was loaded into the pulled glass needle (TW 100F-4, World Precision Instruments, Sarasota, Florida, United States). Injections were performed at three co-ordinates relative to Bregma: (i) 1.5

anterior/posterior (A/P) and 0.7 medial/lateral (M/L); (ii) 1.75 A/P and 0.4 M/L; and (iii) 1.25A/P and 0.1M/L. Each injection was performed at two depths, with 0.5µL being injected at a depth of 0.8mm from the top of the cortex, and a further 0.5µL being injected at a depth of 1.2mm from the surface of the cortex. The injections were performed at a rate of 0.1µL/minute and were controlled using a syringe pump (Fusion 100, Chemyx, Texas, United States), with a 5 minute hold after infusion to prevent back flow. This was repeated for each of the three injection sites. After injections, the needle was removed and three steel sutures were used to pull the skin over the initial incision. 2mL of lactated ringer's solution was given subcutaneously on the rump to prevent dehydration during recovery. The mouse was placed into a cage with food available on the floor as well as being heated on one side for 1-3 hours to prevent hypothermia.

2.3 Tissue collection

2.3.1 Labeling of proliferating cells

To label actively dividing cells on the day of collection, mice were given 4 intraperitoneal injections of bromodeoxyuridine (BrdU, 100µg/g body weight, B5552, Sigma, Ontario, Canada) in two hour intervals. Mice were euthanized 30 minutes following the last BrdU injection.

2.3.2 Perfusion and cryosectioning

Prior to perfusion, the mouse was given a 300µL overdose of sodium pentobarbital. Transcardial perfusion was performed once the mouse was unresponsive. The chest cavity was opened to expose the heart. Once accessible, the right atrium was cut to allow

for blood drainage, and 10mL of chilled phosphate buffered saline pH 7.4 (PBS) was injected into the left ventricle. Subsequently, 20mL of chilled 4% paraformaldehyde pH 7.4 (PFA) was injected through the left ventricle to fix the tissue. Following perfusion brains were dissected and postfixed overnight in 4% PFA. Brains were subsequently cryoprotected using sucrose solution in PBS, changed daily, from 12% (w/v) to 16% (w/v) and 16% (w/v) to 22% (w/v). Brains were frozen in O.C.T. TissueTek mounting medium (25608-930, Sakura Finetek, California, United States) using 2-methylbutane. Brains were cryosectioned (Microm HM520, Thermo Scientific, Ontario, Canada) into 14µm thick coronal sections. Tissue was collected on slides (Superfrost Plus, 12-550-15, Fisher, Ontario, Canada) throughout the A/P extent of the injury.

2.4 Histological staining

2.4.1 Cresyl violet staining

Sections spaced 140µm were selected for cresyl violet staining. Slides were placed on a slide warmer at 37^{o}C for 30 minutes prior to being stained in 0.1% cresyl violet solution (C1791, Sigma, Ontario, Canada) for 45 minutes. Slides were then dehydrated in a series of ethanol/water solutions, (50%(v/v), 70%(v/v), 90%(v/v), 95%(v/v), and 100% (v/v) times 3), followed by isopropanol and toluene prior to coverslipping using Permount (SP15-500, Fisher, Ontario, Canada).

2.4.2 Immunohistochemistry:

2.4.2.1 Fluorescent immunohistochemistry

Three slides were chosen for fluorescent immunohistochemistry (IHC), which previously were identified to be representative of the 1mm A/P range of the centre of the infarct by cresyl violet staining. Slides were placed on a slide warmer at 37^{o}C for 20 minutes and a hydrophobic moat was drawn around the tissue to retain antibody solution (Dako Pen, S200230-2, Dako, Ontario, Canada). For BrdU IHC, slides were post-fixed in acetone for 2 minutes, and subsequently treated with 2N hydrochloric acid for 30 minutes at 37^{o}C to allow nuclear penetration of the antibody, followed by 0.1M sodium borate (pH 8.0) for 10 minutes for neutralization. Subsequently slides were washed in PBS for 20 minutes and incubated overnight with the proper primary antibody (Table 2.1). The following morning slides were washed in PBS for 20 minutes and incubated with the corresponding secondary antibody (Table 2.2) for 1 hour. After incubation slides were washed in PBS for 10 minutes, and counterstained with Hoechst (1:250, BisBenzimide H33258, B1155, Sigma, Ontario, Canada) for 2 minutes, and washed in PBS for 10 minutes. Slides were then coverslipped using 125μL of a 1:3 glycerol:PBS solution.

Table 2.2.1 Primary Antibodies

Specificity	Host	Concentration	Source
BrdU	Mouse	1:100	BD Biosciences 347580
Doublecortin	Goat	1:200	Santa Cruz sc-8066
GFAP	Goat	1:400	Santa Cruz sc-6171
CD-68	Rat	1:400	ABD Serotec MCA1957
Active Caspase 3	Rabbit	1:400	BD Biosciences 559565

Table 2.2.2 Fluorescent Secondary Antibodies

Specificity	Fluorphore	Concentration	Source
Mouse	Alexa Fluor 594	1:200	Invitrogen A21203
Goat	Alexa Fluor 488	1:200	Invitrogen A11055
Rabbit	Alexa Fluor 488	1:200	Invitrogen A21206

2.4.2.2 Immunohistochemistry using enzymatic detection

IHC with enzymatic detection was performed as follows; slides were warmed on a slide warmer for 20 minutes. Slides were then washed in a 100mM Tris HCl pH 7.5 0.15M NaCl solution (Tris buffer) for 20 minutes and a hydrophobic moat was drawn around the tissue to retain antibody solution (Dako Pen, S200230-2, Dako, Ontario, Canada). The slides were incubated in primary antibody overnight (Table 2.1). The following mornings, slides were washed in Tris buffer for 20 minutes, followed by an endogenous peroxidase treatment of 0.3% hydrogen peroxide in methanol. Slides were then washed in Tris buffer for 20 minutes. Following washing the slides were incubated with the

appropriate secondary antibody (Table 2.3). For biotinylated conjugated secondary antibodies, an avidin biotin complex (VECTASTAIN Elite ABC kit (Universal), PK-6200, Vector Laboratories, Ontario, Canada) kit was used to amplify the enzymatic detection. The slides were then washed in Tris buffer for 20 minutes. Slides were then incubated in DAB solution (DAB Peroxidase Substrate Kit, 3,3'-diaminobenzidine, SK-4100, Vector Laboratories, Ontario, Canada) for 5 minutes, until suitable staining developed, then washed in tap water for 5 minutes. Slides were then dehydrated in ethanol as detailed in section 2.4.1 and coverslipped in Permount mounting media (SP15-500, Fisher, Ontario, Canada).

Table 2.2.3 DAB Secondary Antibodies

Specificity	Detection Enzyme	Concentration	Source
Rabbit	Biotinylated	1:200	Jackson 11-065-152
Rat	HRP	1:200	Jackson 112-035-008

2.5 Infarct Volume and Edema Factor analysis

Infarct volume was assessed by imaging cresyl violet slides. Slides were photographed using a Zeiss Axiocam Mrm camera, through a Zeiss stereoscope (Stemi-2000 C, Carl Zeiss Microscopy, Jenna, Germany). Infarct volume was determined by measuring the outline of the infarct on coronal sections at 140µm intervals through the A/P extent of the injury. To achieve this, the area of the cortex contralateral to the injury was compared to the area of healthy cortex on the hemisphere ipsilateral to the injury. Volume was

estimated by integrating the changes in area over the 140µm distance between representative sections, using the equation below:

$$Infarct\ Volume =$$

$$140\mu m\ x\ \sum(Contralateral\ cortical\ area - Healthy\ ipsilateral\ cortical\ area)$$

The infarct volume was corrected for edema. The edema factor was calculated in accordance with literature and multiplied by the infarct volume (Belayev et al., 2005).

$$Edema\ Factor = \frac{total\ ipsilateral\ cortical\ area}{total\ contralateral\ cortical\ area}$$

The corrected infarct volume can then be calculated using the following equation:

$$Corrected\ infarct\ volume$$

$$= 140\mu m\ x\ \sum(\frac{Contralateral\ cortical\ area - Healthy\ Ipsilateral\ cortical\ area}{Edema\ Factor})$$

2.6 Immune cell area of activation

The area of immune cell activation was measured using ImageJ (NIH, http://rsbweb.nih.gov/ij/) and two sections spanning the centre of the injury. Photomicrographs were taken using a Zeiss Axiocam Mrm camera, at 3.2X magnification on a Zeiss stereoscope (Stemi-2000 C, Carl Zeiss Microscopy, Jenna, Germany). Activated immune cells were traced and averaged over the two sections per animal.

2.7 Cell counting

Cell counts were performed using ImageJ (NIH, http://rsbweb.nih.gov/ij/). Nine sections from 3 slides, spanning a 1mm area that spanned the centre of the infarct previously

identified by cresyl violet staining, were selected per mouse for immunohistochemical staining. Photomicrographs were taken using a Zeiss Axiocam Mrm camera at 20X magnification on a Zeiss Imager.Z1 microscope (Zeiss Imager.Z1, Carl Zeiss Microscopy, Jenna Germany). Slides were blinded prior to quantification. Quantification of NPCs within the subventricular zone (SVZ) was completed by quantifying BrdU positive cells along the entire length of the SVZ of the ventricle ipsilateral to the infarct. Quantification of double labelled BrdU and Dcx positively labelled neuroblasts was completed by ensuring co-localization of BrdU and Hoechst in Dcx positive cells along the entire length of the SVZ of the ventricle ipsilateral to the infarct.

2.8 Densitometry analysis

Densitometry was performed using ImageJ software (NIH, Massachusetts, United States). All images were blocked into 62500μm^2 areas. Consecutive representative sections 140 μm apart were used from the centre of the infarcted area as assessed by cresyl violet staining. Rodbard correction (NIH, http://rsbweb.nih.gov/ij/) was used to standardize gray levels for analysis. Five gridded sections were used to measure gray levels within the region of interest. Three areas of interest were used on non-stained gray matter as background control levels. The density of the areas of interest were averaged and then subtracted with the average of the background areas. To assess astrocyte activation, areas were selected along the border of the injury as determined by the lack immunostaining within the injury, and areas at a distance of 250μm lateral to the border of injury.

2.9 Statistical testing

GraphPad Prism 5 (GraphPad Sofware, California, United States) was used to perform all statistical tests. The Student's t-test was used to compare experimental and control conditions of neuroblast survival, with p-value for significance set at 0.05. One-way and two-way Analysis of Variance (ANOVA) tests were used with the Bonferroni post-hoc test to compare the statistical significance between time points for neural precursor population quantification and newborn neuroblast quantification, α-value for significance was set at 0.05.

3 Results

The Vanderluit lab has recently developed a model of ischemic stroke that involves intracortical injections of ET-1 into the mouse forelimb motor cortex (Roome et al., 2014). The goal of this research project was to use this stroke modelto study the progression of the infarct over the first 10 days post-stroke. This included analysis of the volume of the infarct, the cell death profile, and the glial and NPC responses. To specifically understand the NPC response post-stroke, both NPC proliferation and newborn neuroblast levels were assessed. The goal of this strategy was to characterize the acute cellular changes occurring within and surrounding the infarct.

3.1 The infarct volume is consistent over the first 10 days post-injury

To test if the volume of an ischemic injury changed over the first 10 days post-injury, cresyl violet staining was used to differentiate healthy tissue from injured tissue. Cresyl violet stained the endoplasmic reticulum of cells dark purple (Fig. 3.1). When tissue became injured, cells shrunk and the distance between cells increased, this led to areas of pale cresyl violet staining. High magnification of the border between injured and healthy tissue showed the differences between healthy cells and condensed injured cells (Fig. 3.1 A). Areas with small shrunken cells, indicated by white arrows, were judged to be damaged and included in the injury (Fig. 3.1 A). Areas where cells were mainly healthy, indicated by the black arrows, with few dead cells were considered to be not injured (Fig. 3.1 A). Measurements of injured tissue showed sizable injuries in both saline and ET-1 conditions (Fig. 3.1 B-E). Ischemic injuries have a distinctive shape, with injuries flaring

out at the bottom of the cortex (Fig. 3.1 B-E). Saline injuries have a different shape than ischemic injures, with saline injuries being shallower and bowl shaped (Fig. 3.1 B-E). Saline injuries also appear to have fewer pale areas (Fig. 3.1 B-E). Statistical analysis of injury volumes showed that ET-1 induced infarcts were only significantly larger than saline injuries at 7 days post-surgery but not at the other time points (Fig. 3.1 F). Although infarct volumes between ET-1 and saline injuries were not significantly different at all time points; statistical analysis revealed main effects for time. A trend towards smaller infarct volumes for both ET-1 and saline injuries appeared at 10 days versus earlier time points. The edema factor for both ET-1 and saline injuries did not change significantly over time post-surgery, remaining stable at a mean of 1.15 across the time points (Fig. 3.1 G). Although not significant, a trend towards smaller injuries was observed in both ET-1 and saline injuries between the 1st day and the 10th day post-surgery.

Figure 3.1: Infarct volume is stable following initial injury.

A - Representative high magnification (10X) photomicrographs of cresyl violet staining near the border of the injury. Line indicates the border of the injury. Black arrows indicate healthy cells while white arrows indicate small shrunken cells.

B-E - Representative photomicrographs (2.5X) of cresyl violet staining of coronal sections through the cortex of saline and ET-1 injuries at 1 (B), 3 (C), 7 (D) and 10 (E) days post-surgery. Injury areas are traced in black.

F - Quantification of injury volume at 1, 3, 7 and 10 days post-surgery. Data is represented as means plus or minus standard error of the mean (± SEM). Means were analyzed by two-way ANOVA revealing significant effects for treatment [$F(1,23)=13.43$, $p=0.0013$], and time [$F(3,23)=3.358$, $p=0.0363$] then followed by Bonferroni posthoc tests. (1d, n=4 saline, n=4 ET-1; 3d, n=4 saline, n=3 ET-1; 7d, n=4 saline, n=3 ET-1; 10d, n=4 saline, n=5 ET-1). *$p<0.05$. Edema factor was measured for each injury.

G - Quantification of edema factor at 1, 3, 7 and 10 days post-surgery. Data is represented as mean ± SEM. Means were analyzed by two-way ANOVA revealing no significant effects. Dotted line at 1.00 represents the baseline of no edema.

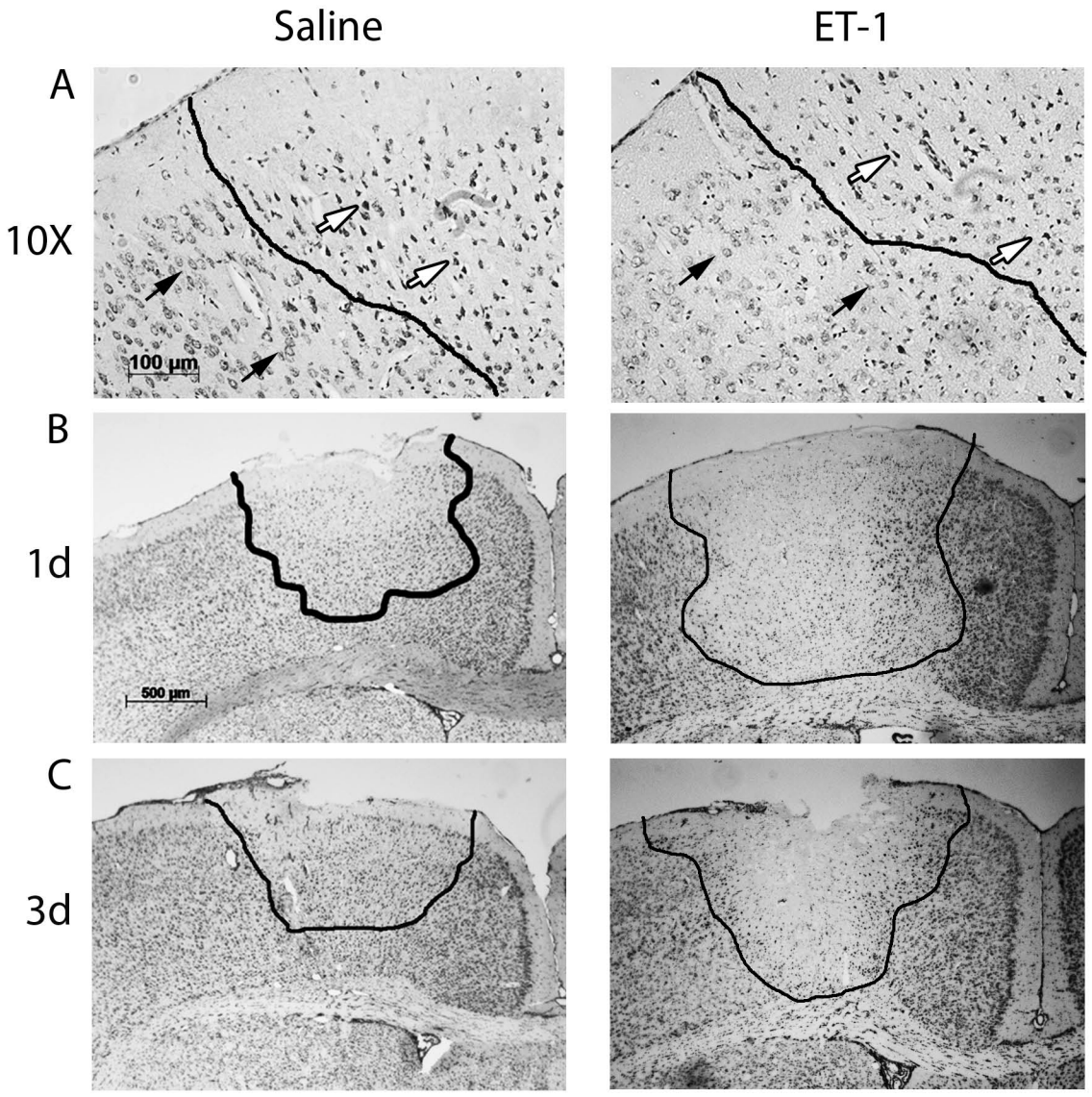
Saline
ET-1
A
10X
100 µm
B
1d
500 µm
C
3d

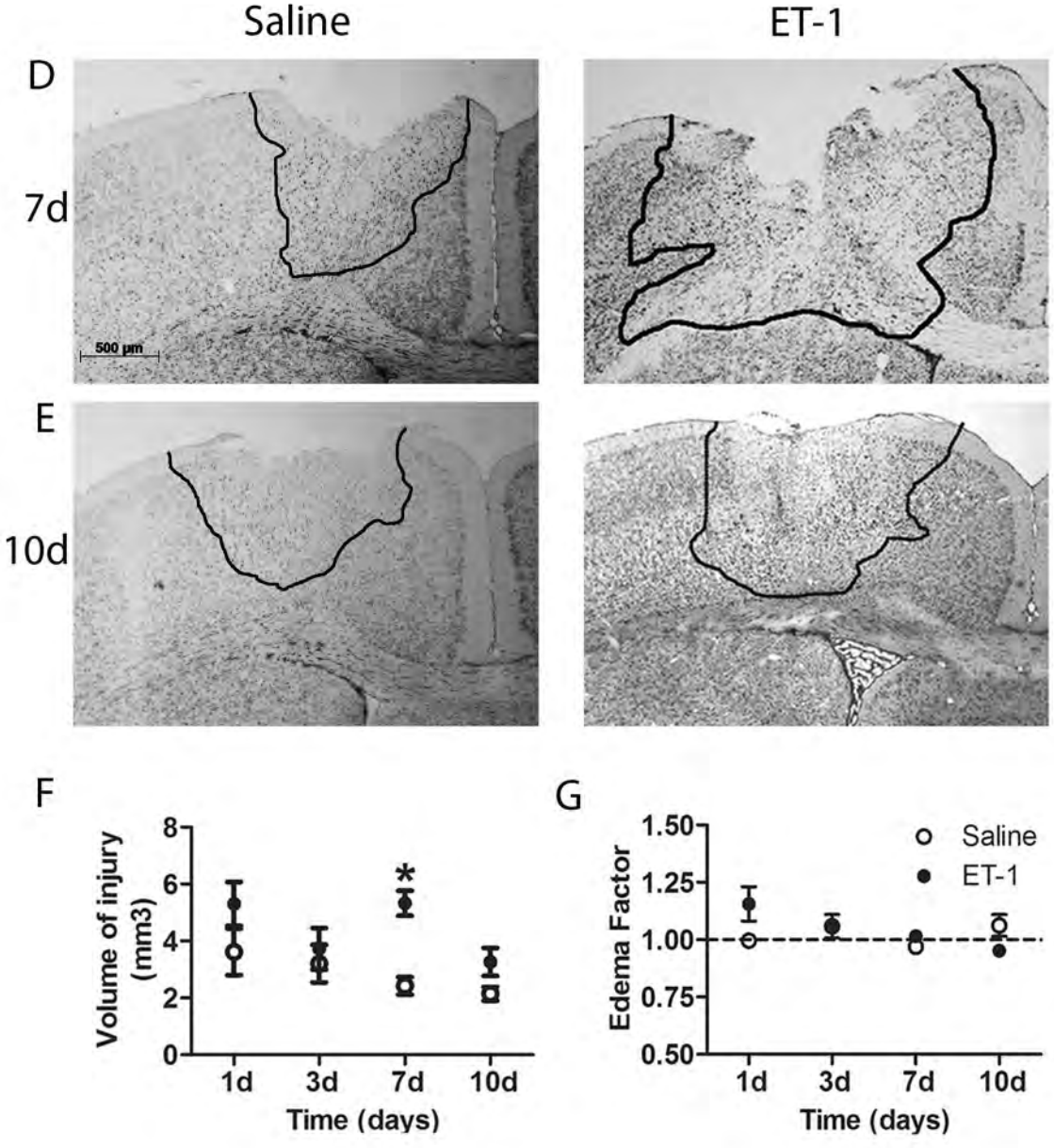
Saline
ET-1
D
7d
500 µm
E
10d
F
Volume of injury (mm3)
8
6
4
2
0
1d
3d
7d
10d
Time (days)
*
G
Edema Factor
1.50
1.25
1.00
0.75
0.50
Saline
ET-1
1d
3d
7d
10d
Time (days)

3.2 Apoptotic cell death occurs up to 3 days post-stroke

To understand how the infarct is formed and the ongoing changes within the post-ischemic cortex, the cellular death response between ischemic and saline injuries was examined. To determine whether apoptotic cell death occurred post-stroke, immunohistochemistry for active caspase 3 was performed. Active caspase 3 is a hallmark of apoptotic cell death. Apoptosis was confirmed using Hoechst, a nuclear cell stain, to visualize condensed apoptotic nuclei. Extensive apoptotic cell death was not observed in either ET-1 or saline injuries. Immunostaining did reveal a few apoptotic cells surrounding the ET-1 induced infarct at 1 and 3 days post-stroke (Fig. 3.2 B,F). Due to the low level of apoptotic cell death, quantification was not performed. Apoptosis appeared to occur in small clusters at 1 day post-stroke. By 3 days post-stroke, fewer apoptotic cells were observed. No apoptotic cell death was detected by immunohistochemistry for active caspase 3 at 7 and 10 days post-stroke (data not shown). Apoptotic cells were not detected in saline injuries at any time point. Although no active caspase 3 positive cells were observed in saline injuries (Fig. 3.2 A,E), high magnification photomicrographs revealed shrunken but not apoptotic nuclei at both 1 and 3 days post-surgery (Fig. 3.2 C,G). This suggests a specific window for apoptosis up to 3 days post-stroke, and it occurs in ischemic injuries but not saline injuries.

Figure 3.2: Apoptotic cell death is seen up to 3 days post-injury.

Immunohistochemical staining for active caspase 3 was performed to label cells undergoing apoptosis. Hoechst, a nuclear stain, was used to confirm apoptotic nuclei. Representative photomicrographs of immunohistochemical staining for active caspase 3 and Hoechst were taken from saline and ET-1 induced injures at 1 and 3 days post-injury.

A,B- Active caspase 3 (AC3) staining at 1 day post-surgery revealed no active caspase 3 staining in saline injuries. However in ET-1 conditions small groups of positively labeled cells can be observed. High magnification (20X) of active caspase 3 positive cells with arrows indicating apoptotic cells (inset).

C,D- Hoechst staining at 1 day post-surgery. The apoptotic nuclear morphology is not observed in cells within saline injuries. In contrast, condensed, apoptotic nuclei are observed in ET-1 injuries. High magnification (20X) of cell nuclei (insets).

E,F- Similarly, at 3 days post-surgery, active caspase 3 positive cells were not observed in saline injuries, whereas, a few active caspase 3 positive cells were observed in ET-1 injuries. High magnification (20X) of AC3 positive cells in the ET-1 injury with an arrow indicating the apoptotic cell (inset).

G,H- Hoechst staining at 3 days post-surgery. The apoptotic nuclear morphology is not observed in cells within saline injuries cells, however, condensed apoptotic nuclei are observed in ET-1 injuries. High magnification (20X) of nuclei (insets). An arrow indicates an apoptotic cell (inset).

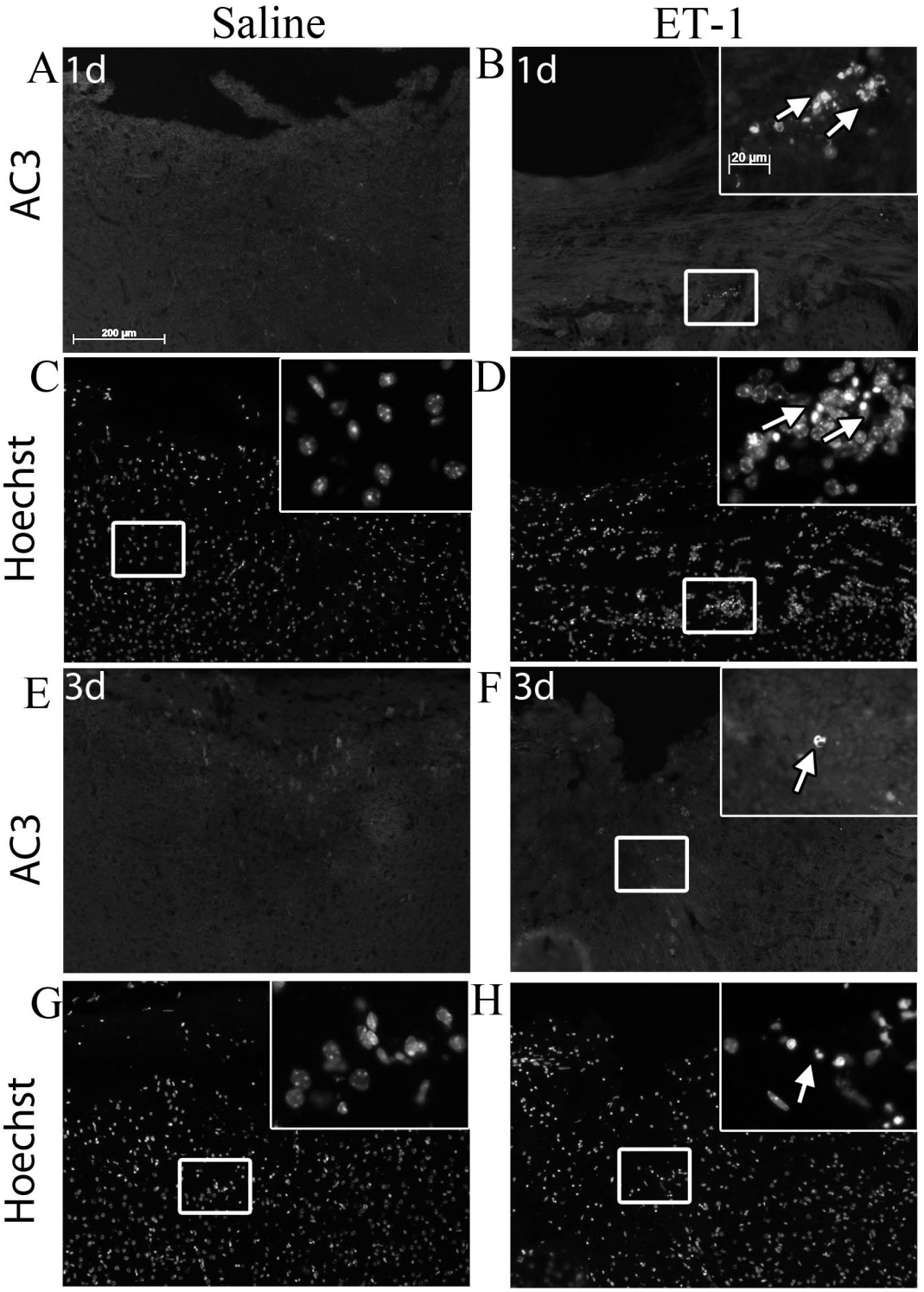
Saline
ET-1
A
1d
AC3
200 µm
B
1d
20 µm
C
Hoechst
D
E
3d
AC3
F
3d
G
Hoechst
H

3.3 Astrocytes are activated surrounding the injury post-stroke

3.3.1 The morphology of astrocytes changes post-ischemic injury.

Immunohistochemistry for GFAP, a marker for astrocytes, was used to compare the morphology of astrocytes in naïve, saline and ischemic brains at 7 days post-injury. Gray matter astrocytes appear to have upregulated GFAP and have larger, swollen cell bodies in both ET-1 and saline brains compared to naïve controls (Fig. 3.3). Additionally, activated astrocytes appear to have more processes than non-activated astrocytes (Fig. 3.3). White matter astrocytes appear to be aligned along the tracts of white matter (Fig. 3.3). These hallmark characteristics including swollen cell bodies, increased number of processes and upregulated GFAP expression were used to differentiate activated from non-activated astrocytes.

Figure 3.3: Morphological changes associated with astrocyte activation post-stroke.

Representative photomicrographs of GFAP immunohistochemical staining of naïve, saline and ET-1 treated brains at 7 days post-surgery. Activated astrocytes residing in gray matter appear to have an increased number of processes in both ischemic and saline conditions. Activated astrocytes residing in white matter appear swollen compared to naïve conditions in both saline and ET-1 conditions. In ET-1 conditions distinct processes can be seen in white matter astrocytes. Arrows indicate increased processes on activated astrocytes.

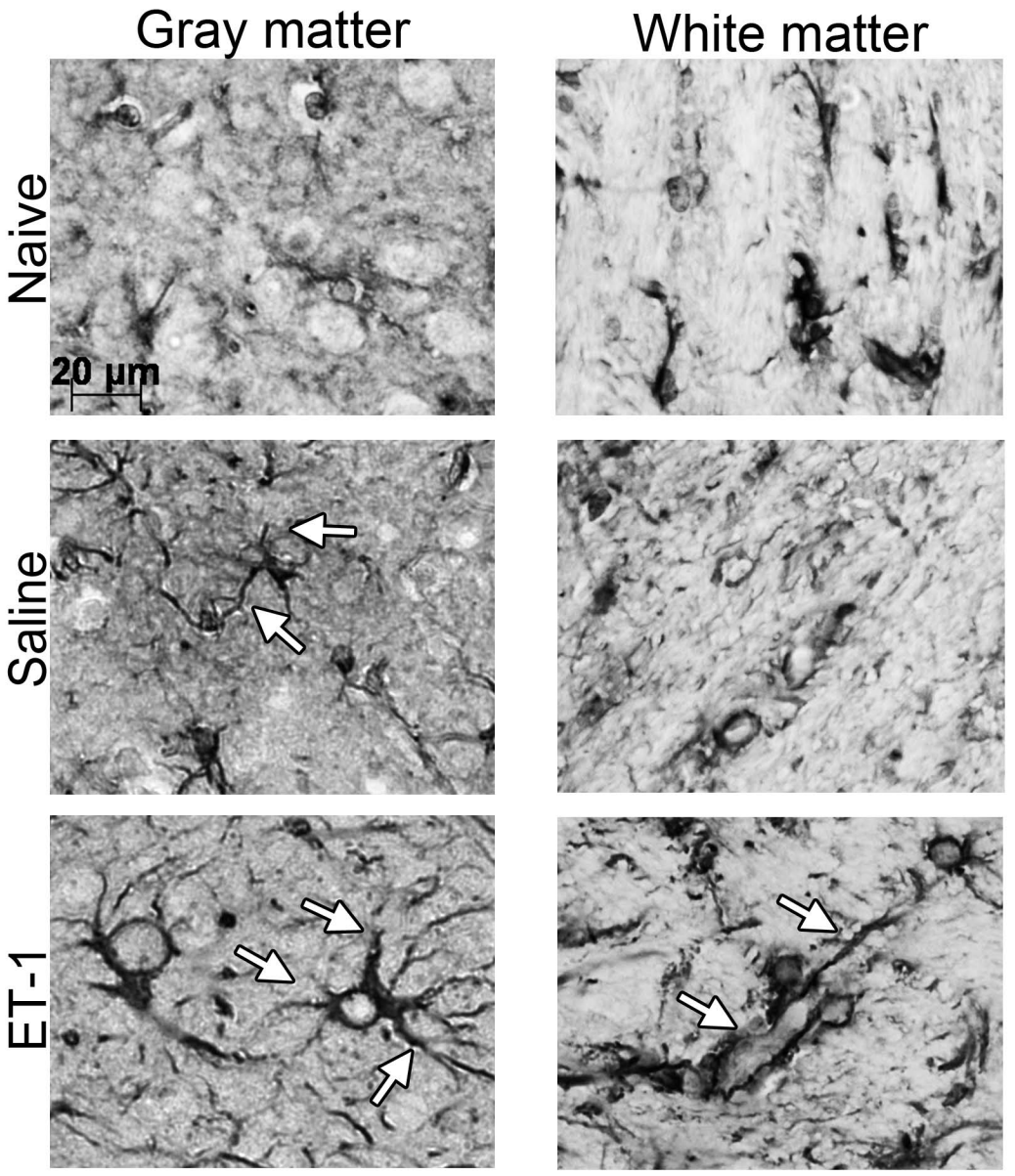
Gray matter
White matter
Naive
Saline
ET-1
20 µm

3.3.2 Activation of astrocytes spreads across the ischemic cortex.

Glial scars play a sizable role in shaping the post-ischemic cortex by forming a barrier to contain ROS and extracellular glutamate and by secreting pro-survival factors (Deb et al., 2010). Therefore, understanding when and how astrocytes respond to a focal ischemic injury can potentially be used to provide an optimal target window for interventional therapies. Immunohistochemistry for GFAP, revealed activated astrocytes in both ET-1 and saline injuries (Fig. 3.3). When all time points are viewed there appears to be a progression of astrocyte activation across time in both saline and ET-1 injured brains. At 1 day post-surgery, there is some astrocyte activation surrounding the sites of injury (Fig 3.4A,B). By 3 days post-surgery, activated astrocytes can be seen outside the site of injury and there appears to be a lack of GFAP immunostaining within the injury (Fig 3.4C,D). By 7 days post-surgery, activated astrocytes appear to have spread across the ipsilateral hemisphere in both saline and ET-1 injured brains (Fig 3.4E,F). In ET-1 injured brains, astrocyte activation was also observed in the contralateral hemisphere (Fig. 3.4F). By 10 days post-surgery, GFAP immunostaining appears reduced in saline treated brains whereas intense GFAP immunostaining is still observed in the ipsilateral hemisphere in ET-1 injured brains (Fig. 3.4G,H). However, astrocyte activation is no longer observed in the contralateral hemisphere in ET-1 injured brains at this time point. This decrease in astrocyte activation at 10 days post-surgery may suggest a possible start of the resolution of astrocyte activation.

By 7 days post-surgery, astrocyte activation appears to have spread across the ischemic cortex into the contralateral cortex (Fig. 3.4F, 3.5B). At the same time point in saline

treated brains, activated astrocytes were seen near the ischemic injury, but few activated astrocytes were seen in the contralateral cortex (Fig. 3.5A). This is in contrast to ET-1 treated brains, where numerous activated astrocytes are observed in the contralateral cortex in 3 out of 4 animals examined (Fig.3.5B). This characterization of astrocyte activation shows that astrocytes may respond differently to a saline-mediated injury versus an ischemic injury.

Figure 3.4: Ischemia induces widespread astrocyte activation in the injured cortex.

Representative photomicrographs of brain sections showing immunohistochemical staining for GFAP, which is upregulated during astrocyte activation in saline and ischemic injuries at 1, 3, 7 and 10 days post-injury.

A,B- At 1 day post-injury saline and ET-1 induced injuries show GFAP staining at the site of injury and along the border of the injury.

C,D- At 3 days post-injury saline and ET-1 injuries show GFAP staining at the border of the injury but minimal staining in the core of the injury.

E,F- At 7 days post-injury saline injuries show GFAP staining at the border and in the ipsilateral cortex to the injury. However, at 7 days post-injury in the ET-1 condition robust GFAP staining can be seen in the contralateral cortex in addition to staining throughout the ipsilateral cortex. Arrow indicates GFAP staining in the contralateral cortex.

G,H- At 10 days post-injury saline induced injuries show GFAP staining primarily at the site of injury. In ET-1 induced injuries GFAP staining is observed throughout the ipsilateral cortex but no longer is GFAP staining observed within the contralateral cortex.

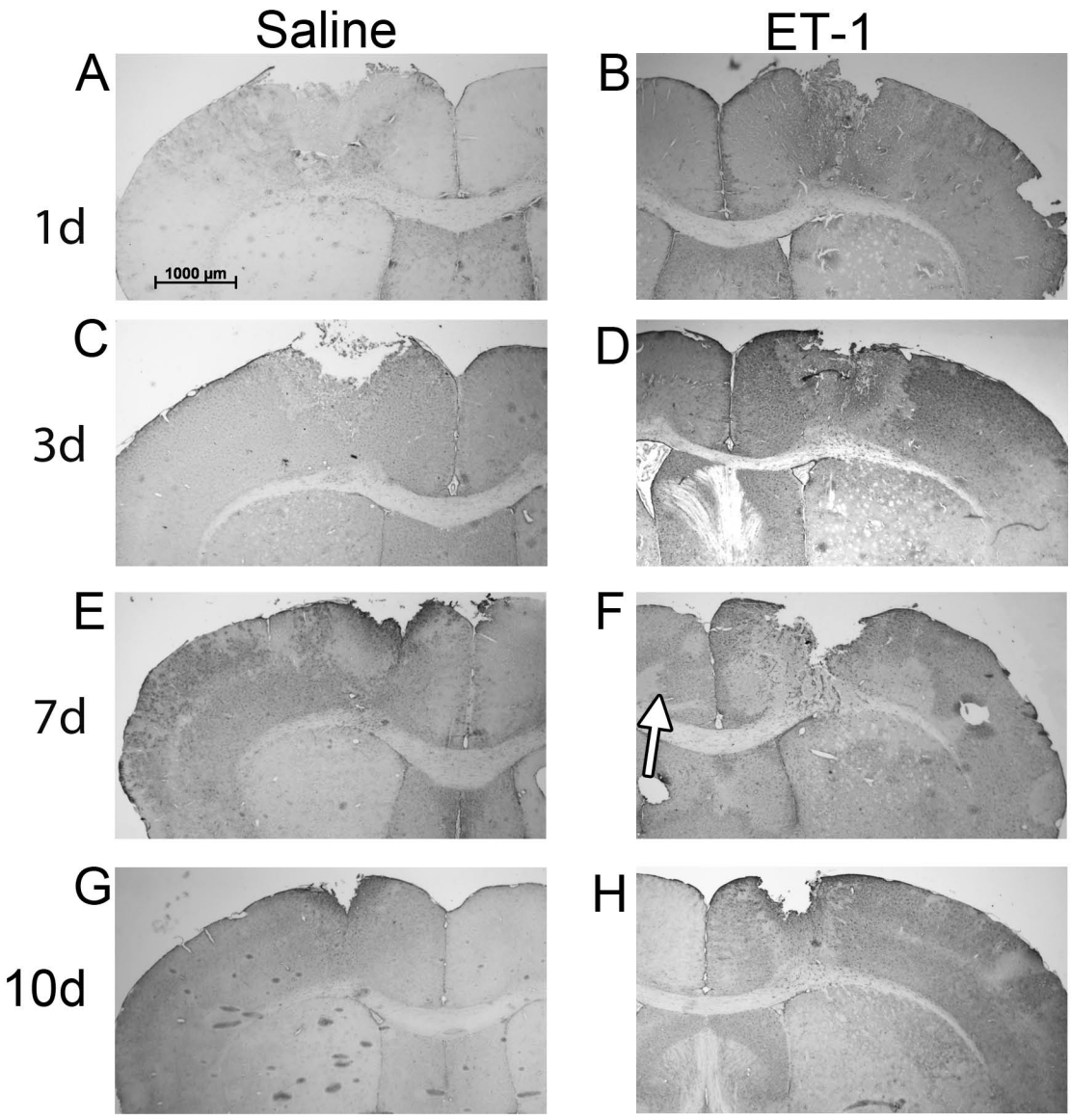
Saline
ET-1
A
B
1d
1000 µm
C
D
3d
E
F
7d
G
H
10d

Figure 3.5: Activation of astrocytes in the contralateral cortex at 7 days post-surgery.

Representative photomicrographs of coronal brain sections showing immunohistochemical staining for GFAP, which is upregulated by activated astrocytes.

A- Representative low magnification (1.25X) of a brain section from a saline induced injury. A` shows high magnification (20X) of the ipsilateral cortex where activated astrocytes are observed. A`` shows high magnification of the contralateral cortex and shows no significant GFAP staining.

B- Representative low magnification (1.25X) of a brain section from a ET-1 induced injury. B` high magnification (20X) of the ipsilateral cortex, where numerous activated astrocytes are observed. B`` high magnification of the contralateral cortex, where activated astrocytes are observed.

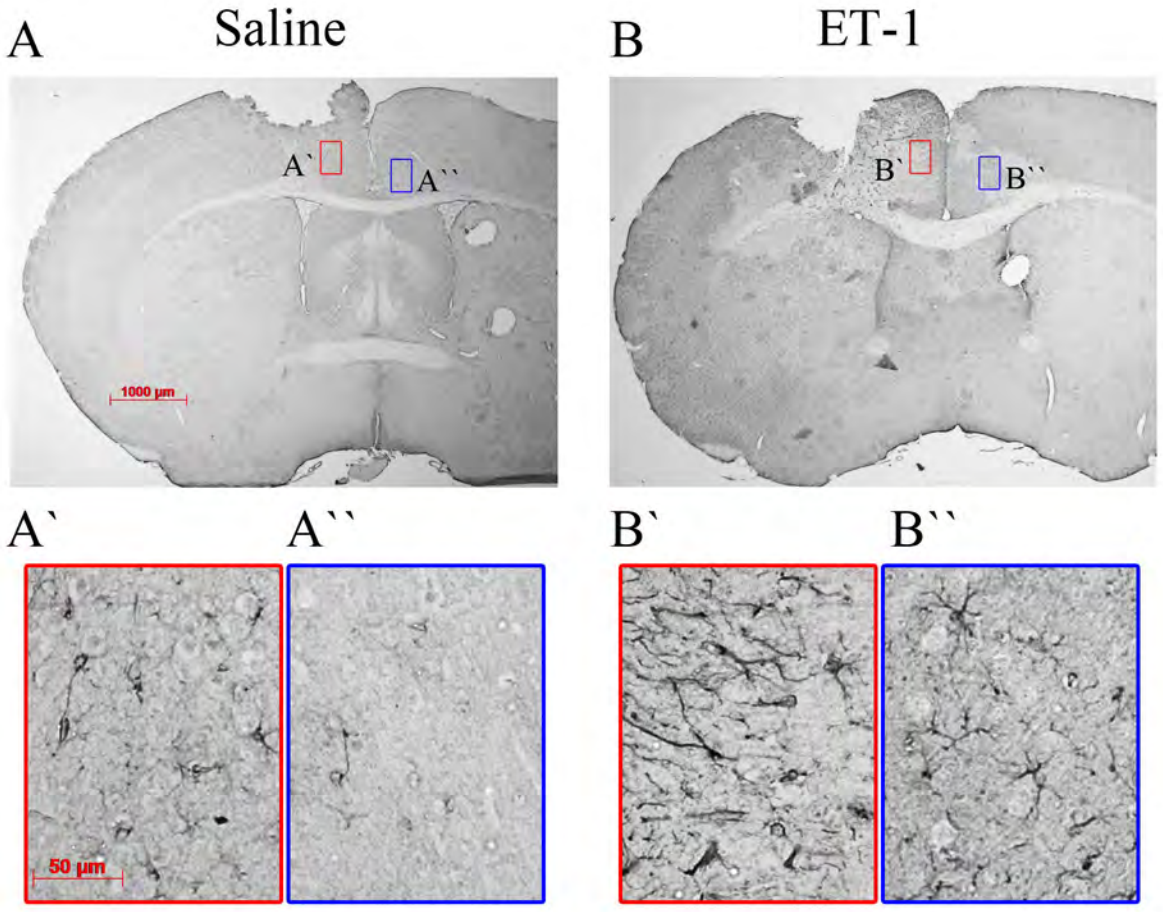
A
Saline
B
ET-1
A`
A``
B`
B``
1000 µm
50 µm

3.3.3 Densitometry of GFAP shows ischemic injuries have a greater spread of astrocyte activation than saline injuries.

To assess astrocyte activation surrounding saline and ET-1 injuries, densitometry of GFAP immunostaining was performed in two areas, at the border of the ischemic injury and 250μm from the injury border (Fig. 3.6 A). GFAP densitometry showed no significant difference between levels of activation surrounding the site of injury between ET-1 and saline injuries (Fig. 3.6 B). Statistical analysis of astrocyte activation 250 μm from the border of the injury revealed main effects for treatment and interaction. Specifically at 7 days post-surgery, there was higher GFAP upregulation 250 μm from the border of the injury in ET-1 injuries compared to saline injuries (Fig 3.6 C). Therefore while saline injuries do cause astrocyte activation surrounding the injury at similar levels to ET-1 mediated injuries, the activation further from the site of injury is stronger in ET-1 mediated injuries at 7 days post-surgery.

Figure 3.6: Densitometry shows the spread of astrocyte activation across the injured cortex.

A- Densitometry of GFAP staining was performed on representative photomicrographs of brain sections at 1, 3, 7 and 10 days post-injury. Red boxes show areas of measurement along the border of the ischemic injury and green boxes show areas of densitometry measured 250µm from the border of the injury.

B- Quantification of GFAP densitometry, at the border of the injury (red boxes). Means were analyzed by two-way ANOVA revealing no significant effects.

C- Quantification of GFAP densitometry from areas 250µm from the border of the injury (green boxes). Means were analyzed by two-way ANOVA revealing main effects for treatment [$F(1,24)=4.640$, $p=0.0415$] and interaction [$F(3,24)=3.059$, $p=0.0476$] then followed by Bonferroni posthoc tests. (1d, n=4 saline, n=4 ET-1; 3d, n=4 saline, n=3 ET-1; 7d, n=4 saline, n=4 ET-1; 10d, n=4 saline, n=5 ET-1). *$p<0.05$

A

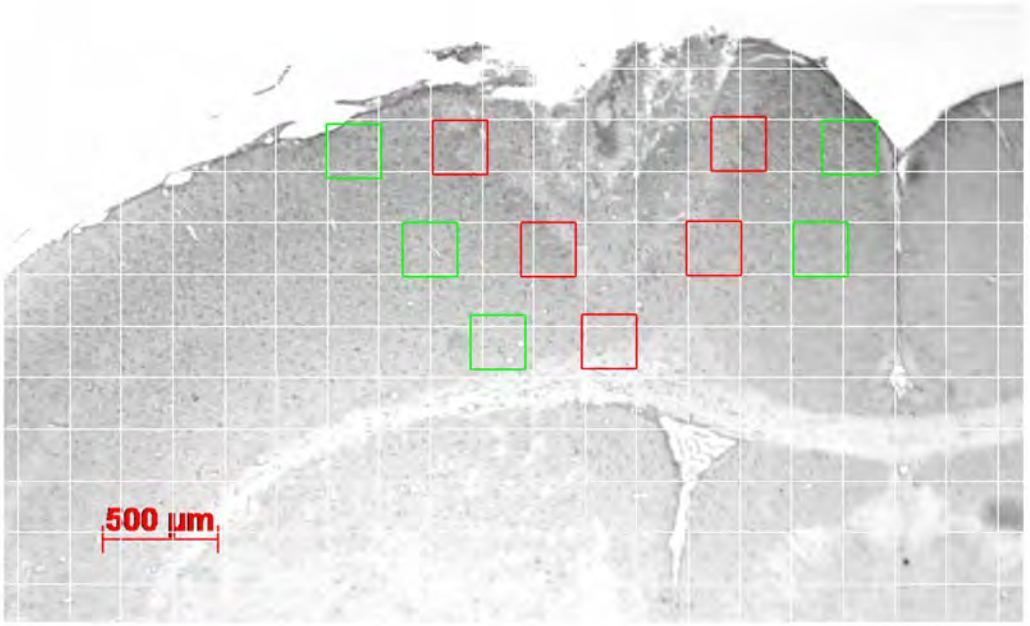
500 µm

B

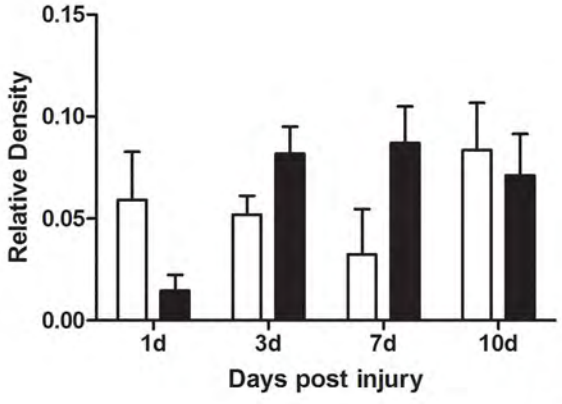
0.15
0.10
0.05
0.00
Relative Density
1d
3d
7d
10d
Days post injury

C

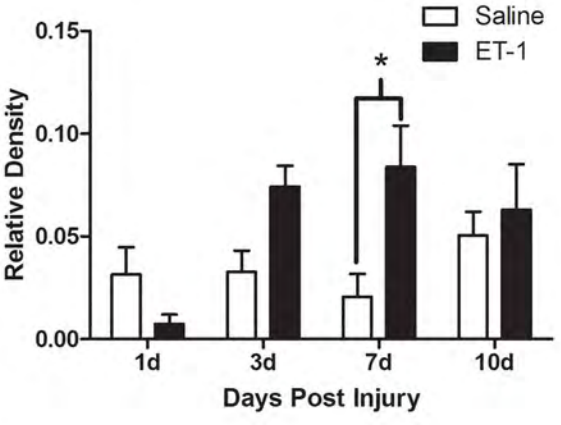
Saline
ET-1
*
0.15
0.10
0.05
0.00
Relative Density
1d
3d
7d
10d
Days Post Injury

3.4 Immune cells are activated within the injury over the first 10 days post-stroke

Along with activated astrocytes, the immune system is part of the glial response to stroke. Understanding when and where immune cells are activated post-stroke allows for testing the role of the immune system in modulating the NPC response. To examine the immune response, immunohistochemistry was performed to detect activated microglia and macrophages. Specifically, antibodies to CD-68, a cell surface marker of activated microglia and macrophages, were used (Slepko & Levi, 1996). Brain sections were selected from the centre of the injury. A few CD-68 positive cells were observed within the infarct at 1 day post-surgery as shown in insets in saline and ET-1 treated brains (Fig 3.7 A,B). By 3 days post-surgery however, robust expression of CD-68 was observed in both saline and ET-1 treated brains (Fig. 3.7 C,D). In contrast to the location of astrocyte activation, CD-68 immunostaining was confined to the site of injury. The spread of CD-68 immunostaining appeared restricted to the core of the injury at 7 and 10 days post-surgery in both saline and ET-1 injured brains (Fig. 3.7 E-H). Cells that were activated by 10 days post-injury were localized to the area surrounding the centre of the infarct (Fig. 3.7 G,H).

Although robust immune cell activation was first observed 3 days post-stroke, the expression of CD-68 positive cells was wide spread across the injury. To assess changes in the spread of CD-68 positive cells within the injury across time post-surgery, the area of CD-68 immunopositive cells was analyzed. At 3 and 7 days post-surgery, there was a significantly larger area of CD-68 positive cells in ET-1 injured brains compared to saline

injured brains (Fig. 3.8 A). By 10 days post-surgery, the area of CD-68 activation was reduced and no longer significantly different from saline treated brains (Fig. 3.8 A).

Next, densitometry of CD-68 was performed to assess the levels of microglia and macrophage activation within the injury. No significant differences were found between groups across the different time point post-surgery (Fig. 3.8B). Densitometry was not performed at 1 day post-surgery because CD-68 immunostaining was below detection levels in both ET-1 and saline treated brains. Overall our results suggest that the immune response to an ET-1 induced injury peaks at day 3-7 post-surgery, then subsides by day 10 to levels similar to that of the saline group. The areas of activated immune cells, when compared to the infarct area, were similar to the corresponding infarct areas.

Figure 3.7: Ischemic injury causes a robust innate immune response.

Representative photomicrographs of brain sections showing immunohistochemical staining for CD-68, a marker for activated microglia and macrophages, in saline and ischemic injuries at 1, 3, 7 and 10 days post-injury. Areas of activated immune cells are outlined in black.

A,B- At 1 day post-injury few CD-68 positive cells were observed located proximal to the needle tract (inset) in both saline and ET-1 conditions.

C,D- At 3 days post-injury robust activation of microglia and macrophages was first detected at 3 days post-injury in both saline and ET-1 induced injuries.

E,F- Robust CD-68 staining continued at 7 days post-injury in both saline and ET-1 induced injuries.

G,H- At 10 days post-injury CD-68 staining is found in close proximity to the needle tract in both saline and ET-1 induced injuries.

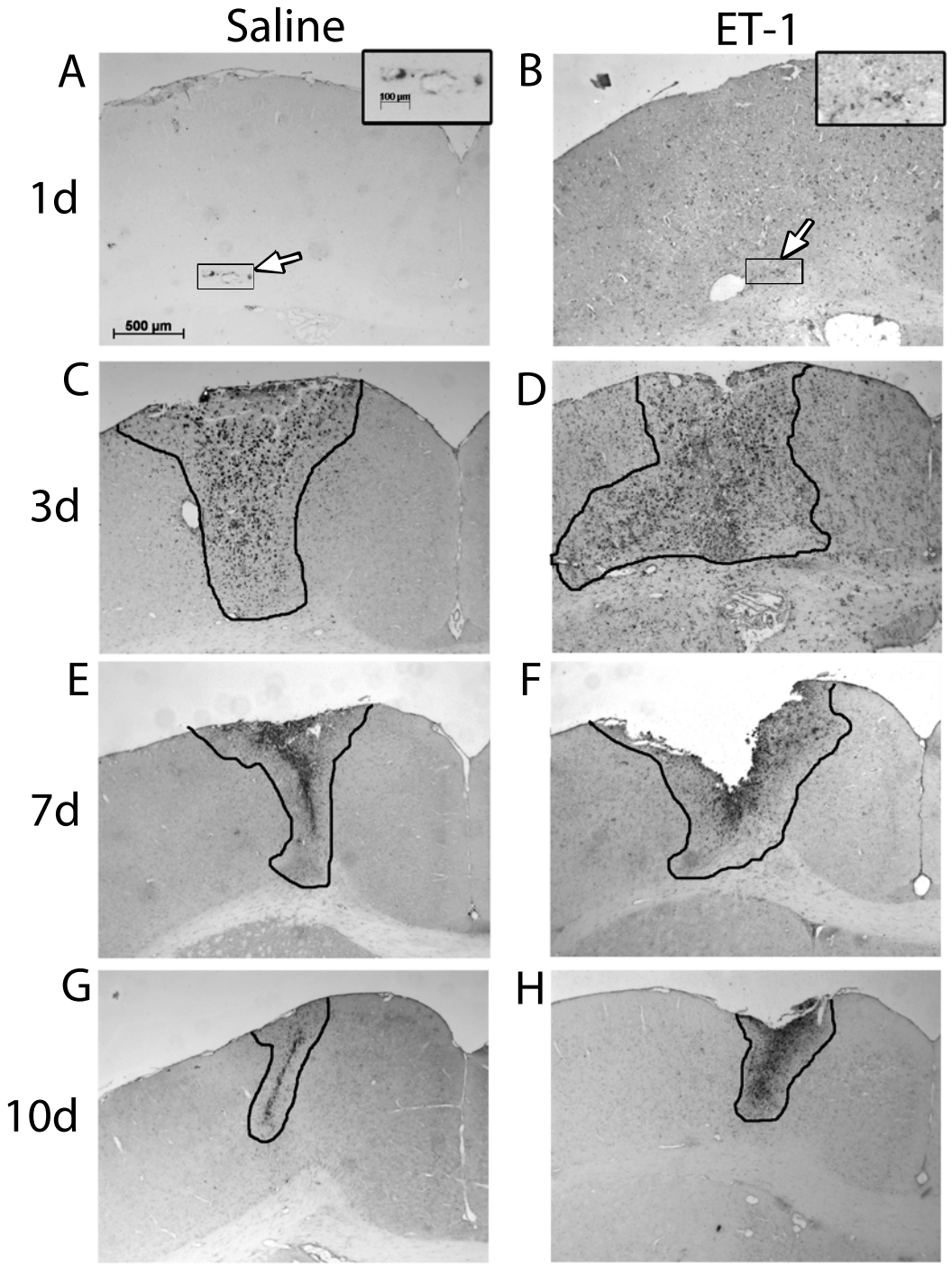
Saline
ET-1
A
B
1d
100 µm
500 µm
C
D
3d
E
F
7d
G
H
10d

Figure 3.8: Microglia and macrophages have a larger response to ischemic injuries than saline over the first 10 days post-injury.

A- The area of CD-68 activation was measured on representative photomicrographs of brain sections at 3, 7 and 10 days post-surgery. Red outline shows the area of CD-68 activated cells. Means were analyzed by two-way ANOVA revealing significant main effects of treatment [$F(1,18)=28.02$, $p<0.0001$], time [$F(2,18)=6.972$, $p=0.0057$] and interaction [$F(2,18)=6.362$, $p=0.0081$] then followed by Bonferroni posthoc tests. *$p<0.05$, ***$p<0.001$.

B- Densitometry of CD-68 was performed on representative photomicrographs of brain sections at 3, 7 and 10 days post-injury. Red boxes show areas for density measurements within the injury. Means were analyzed by two-way ANOVA and showed no significant effects. (1d, n=4 saline, n=4 ET-1; 3d, n=4 saline, n=3 ET-1; 7d, n=4 saline, n=4 ET-1; 10d, n=4 saline, n=5 ET-1).

A

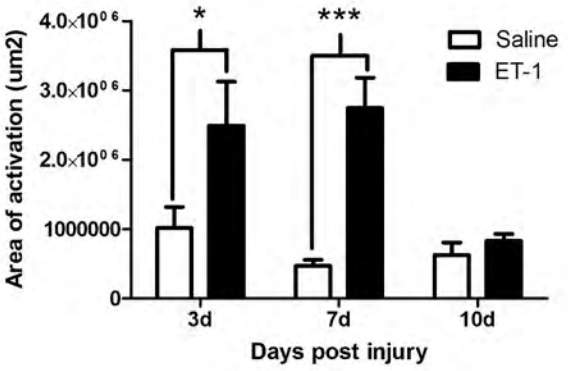
Area of activation (um2)
4.0×10^0 6
3.0×10^0 6
2.0×10^0 6
1000000
0
*
***
Saline
ET-1
3d
7d
10d
Days post injury

B

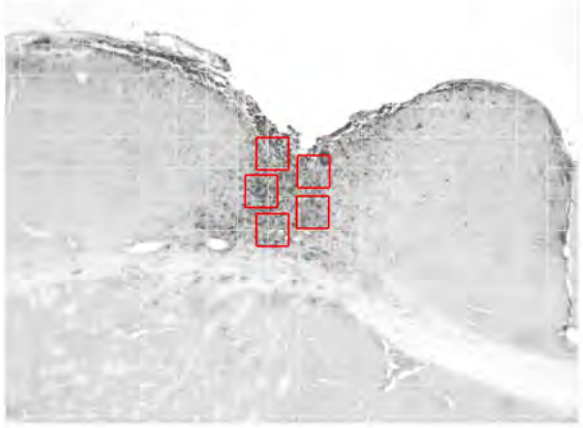

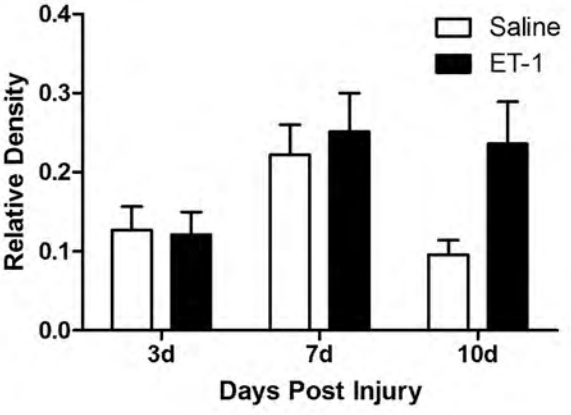
Relative Density
0.4
0.3
0.2
0.1
0.0
Saline
ET-1
3d
7d
10d
Days Post Injury

3.5 Neural precursor cell proliferation changes over the first 10 days post-stroke

To study the impact of a small focal ischemic injury on the proliferative status of NPCs, BrdU was used as a marker for proliferating cells in the SVZ. BrdU is a thymidine analog that is taken up by cells during the S-phase of the cell cycle. BrdU injections labeled the proliferative population of the SVZ for 6 hours prior to sacrifice. Statistical analysis of NPC proliferation within the SVZ ipsilateral to the injury did not reveal any significant differences between saline and ET-1 treatments over the first 10 days post-injury (Fig 3.9 B).

Figure 3.9: NPCs proliferate within the SVZ over the first 10 days post-surgery.

A- Representative photomicrographs of sections from saline and ET-1 treated brains showing BrdU labeled cells within the SVZ at 1, 3, 7 and 10 days post-surgery. The choroid plexus resides within the lateral ventricle fluoresces due to nonspecific staining.

B- Quantification of the total number of BrdU positive SVZ cells over a 1120 μm A/P distance through the centre of the infarct. Data is presented as mean ± SEM. Dotted line represents basal proliferation levels in naïve age-matched controls. Error bars at the one day time point for ET-1 conditions are not visible due to the low variance seen at that time point (SEM=4124.658). Means were analyzed by two-way ANOVA and revealed a significant main effect for time, due to the surgical procedure [$F(3,24)=3.019$, $p=0.0495$]. (1d, n=4 saline, n=4 ET-1; 3d, n=4 saline, n=3 ET-1; 7d, n=4 saline, n=4 ET-1; 10d, n=4 saline, n=5 ET-1; n=3 naïve).

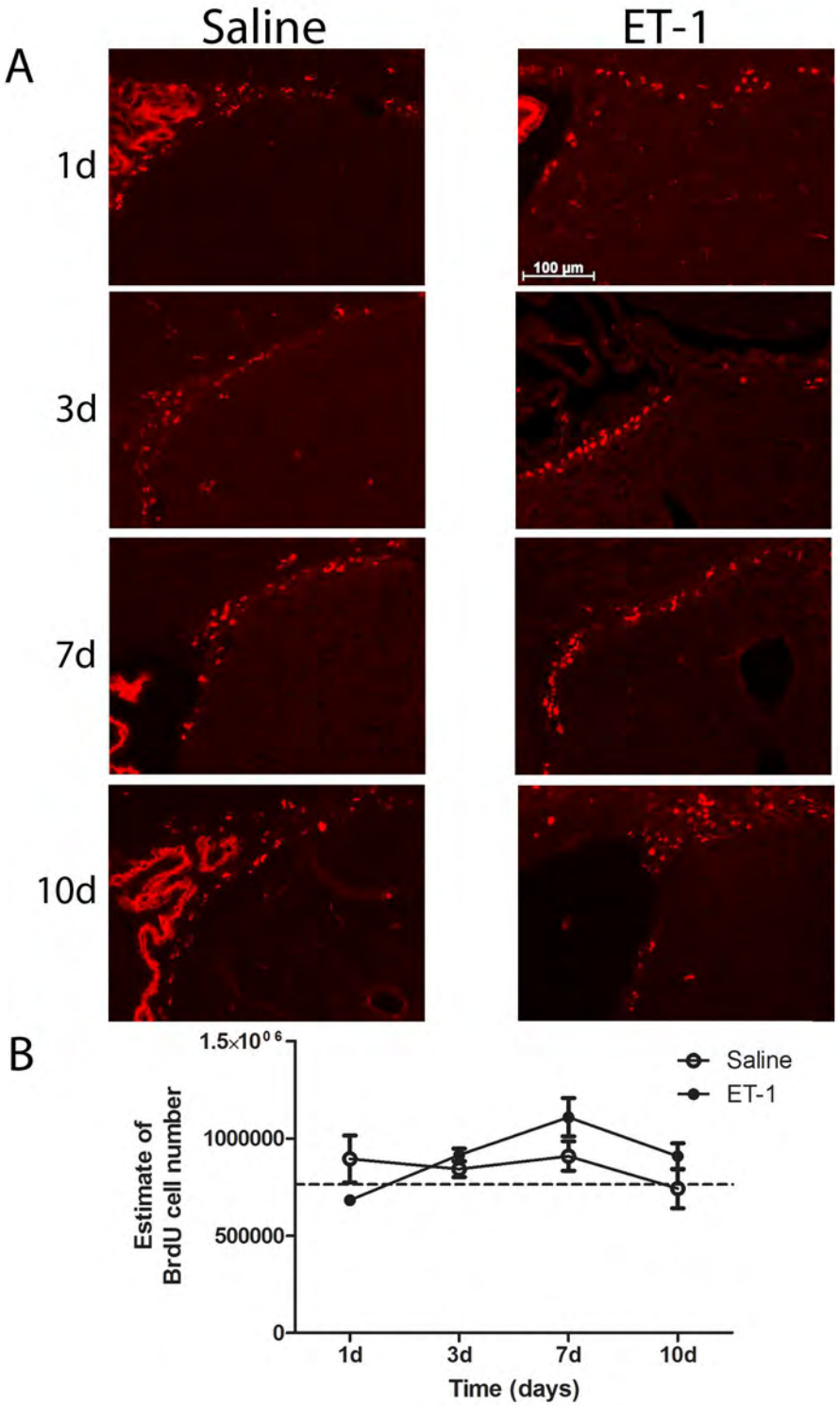
Saline
ET-1
A
1d
3d
7d
10d
100 µm
B
1.5×10^06
1000000
500000
0
Estimate of BrdU cell number
1d
3d
7d
10d
Time (days)
Saline
ET-1

3.6 Newborn migratory neuroblasts are selectively increased at 7 days post-stroke

One of the most well studied subpopulations of NPCs post-stroke is the neuroblast population. Neuroblasts migrate away from the SVZ towards the site of injury (A. Arvidsson et al., 2002). To assess if there was a change in the number of newborn neuroblasts, immunohistochemistry was performed for doublecortin (Dcx), a marker for migratory neuroblasts and BrdU (Gleeson, Peter T, Flanagan, & Walsh, 1999). Cells double positive for Dcx and BrdU were considered the newborn neuroblast population and quantified within the SVZ (Fig.3.10 A). Statistical analysis of the mean estimated number of newborn neuroblasts revealed significantly higher numbers in ET-1 treated brains (363,626.7) versus saline treated brains (208,320.0) at 7 day post-surgery (Fig. 3.10 B). An overall increase in only Dcx positive cells was also observed in both saline and ET-1 treated brains (Fig. 3.10 A). These cells are not actively proliferating within the SVZ and have the potential to migrate towards the site of injury. Although attempted, quantification of Dcx positive cells appeared unreliable due to the high expression of doublecortin in cell processes and difficulty clearly identifying individual cells bodies.

Figure 3.10: Significant increase in the number of newborn neuroblasts 7 days after ischemic injury.

A- Representative photomicrographs of brain sections showing BrdU and Dcx double labeled cells (arrows) in the SVZ of naïve, saline and ET-1 treated brains 7 days post-surgery.

B- Quantification of the number of newborn neuroblasts shows a significant increase in numbers within the SVZ in ET-1 treated brains at 7 days post-stroke. Data is presented as mean ± SEM. Dotted line represents basal newborn neuroblast levels from naïve age-matched controls (n=3). Means were analyzed by two-way ANOVA revealing significant effects of treatment [$F(1,23)=5.324$, $p=0.0304$], time [$F(3,23)=7.614$, $p=0.0010$] and interaction [$F(3,23)=4.827$, $p=0.0095$] then followed by Bonferroni posthoc tests. (1d, n=4 saline, n=4 ET-1; 3d, n=4 saline, n=3 ET-1; 7d, n=4 saline, n=3 ET-1; 10d, n=4 saline, n=5 ET-1). **$p<0.01$

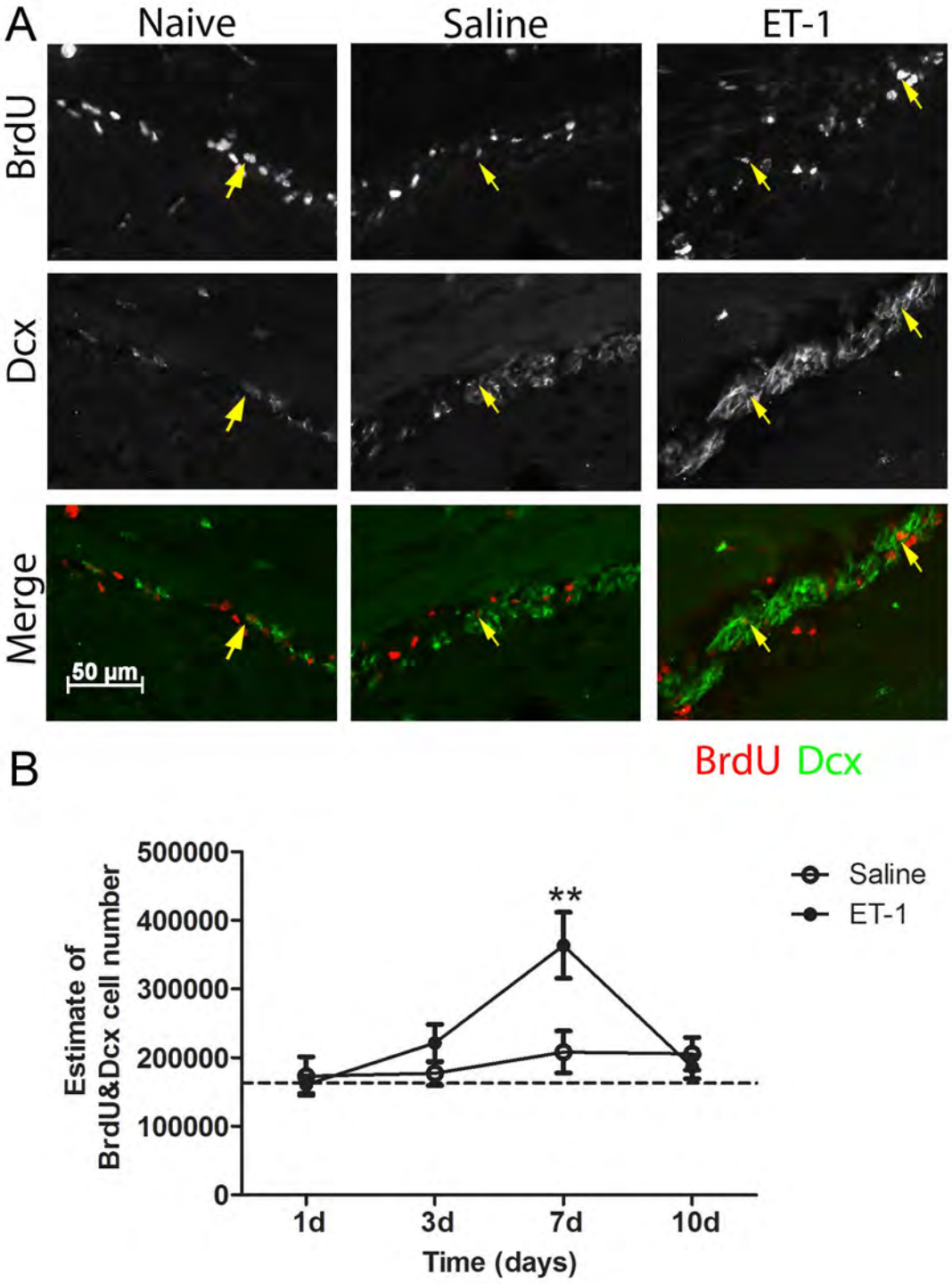
A
Naive
Saline
ET-1
BrdU
Dcx
Merge
50 μm
B
BrdU Dcx
Estimate of BrdU&Dcx cell number
500000
400000
300000
200000
100000
0
**
1d
3d
7d
10d
Time (days)
Saline
ET-1

4 Discussion

4.1 Major findings in this thesis

This thesis has followed the endogenous responses of the mouse brain to a small focal ischemic injury. This has included the characterization of glial and NPC responses over the first 10 days post-stroke. The major findings from this thesis include the stability of the injury size over that time. Another major finding was the progression of astrocyte activation across the injured hemisphere following both ET-1 and saline injections. However, astrocyte activation in the contralateral cortex was primarily observed following an ischemic injury. Immune cell activation was delayed, however, by three days a robust response was observed within the injury site. This is depicted by the spread of activated astrocytes in black and immune cells in red in figure 4.1. In contrast to the characterization of the glial cell responses, the overall proliferative NPC response did not change over the first 10 days post-surgery. However, a significant increase in the newborn neuroblast population, a subset of the NPC population, occurred at 7 days post-stroke. This is demonstrated by the increase in the green cells in figure 4.1. Taken together, the findings in this thesis have identified and characterized the endogenous cellular responses to a new model of small focal ischemic injuries.

Figure 4.1: Endogenous responses to a small focal ischemic injury.

Cartoon representation of the progression of the endogenous cellular responses to a small focal ischemic injury over the first 10 days post-stroke. The spread of astrocyte activation is specifically shown across the ischemic cortex, which was observed at 7 days post-stroke. The delayed immune response is demonstrated with the activated immune cells being confined within the core of the injury. Additionally, the newborn neuroblast peak levels across the first 10 days was observed at day 7 post-surgery. Together, this depicts a highly dynamic situation over a large area of the brain from a small focal ischemic injury.

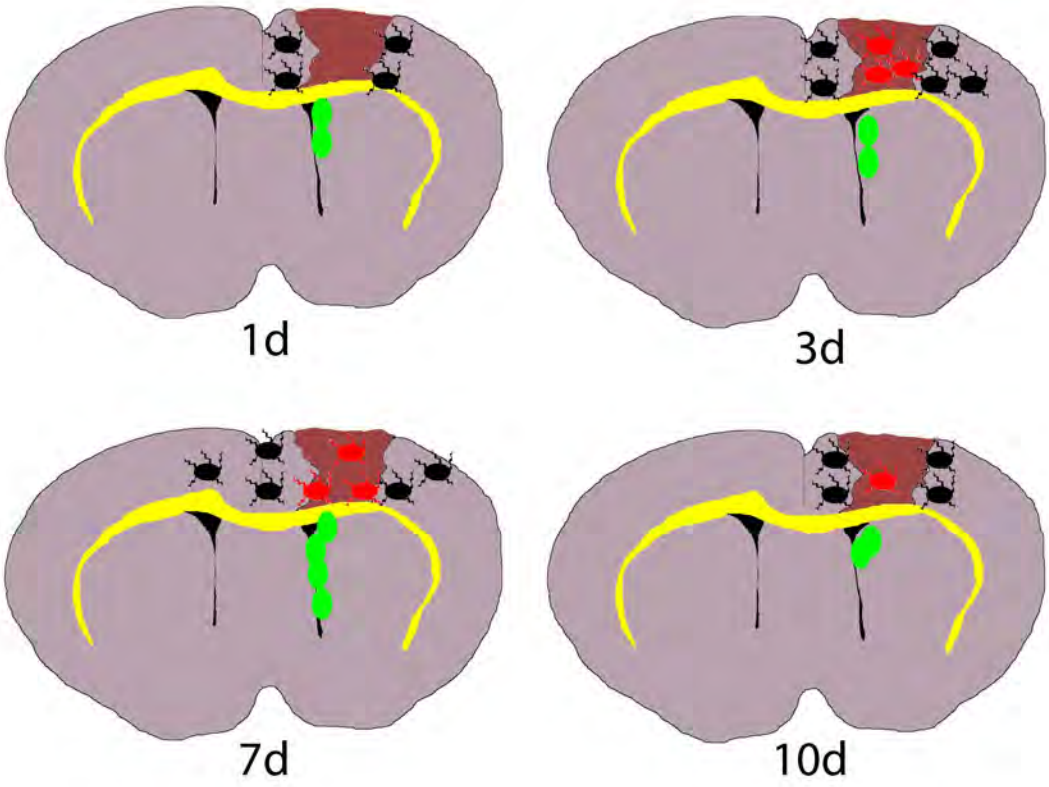
1d
3d
7d
10d


Neuroblasts
Immune cells
Astrocytes

4.1.1 Minor fluctuations in ET-1 ischemic injury size over the first 10 days post-stroke.

The size of the injury was relatively stable across the first 10 days post-stroke. However, a significant increase in infarct volume was observed at 7 days post-stroke which was reduced by 10 days post-stroke. One of the limitations of this study was the low sample sizes of 3-5 animals per time point. This low sample size could lead to increased variance. Although there was no overall change in the size of the infarct between the first day and tenth day post-stroke, an overall trend towards smaller injury volumes were observed. These minor changes in injury volumes across the first 10 days post-stroke are consistent with focal size of the injury and small amount of accompanying edema. This contrasts with other models of ischemic injury. The MCAo model creates a much larger infarct that results in greater edema. Over the first week post-stroke edema resolves and the injury shrinks (Kuraoka, Furuta, Matsuwaki, & Omatsu, 2009). This shrinkage in MCAo injuries causes a change in corrected infarct volume from 20% to 10% between 1 day and 8 days post-stroke (Kuraoka et al., 2009; Lehrmann, Christensen, Zimmer, Diemer, & Finsen, 1997). Therefore, edema following MCAo injuries is a main contributing factor for changes in injury volume. In contrast in this study following an ET-1 mediated stroke, the level of edema was small, with an average edema factor of 1.15, resulting in minimal impact on infarct volume. In human stroke, the primary cause of death in large malignant strokes is inflammation of the brain, a large component of the inflammation is edema which comprises over 30% of the infarct volume (Kasner et al., 2001). Although there are strong similarities with the level of edema between MCAo

injuries and malignant strokes, the high mortality with malignant strokes suggest little can be done. In contrast, the smaller injury size of the ET-1 model is more consistent with focal strokes in humans in which treatment strategies are possible. The ET-1 model therefore, may have more clinical relevance to test therapeutic treatments.

In this ET-1 mediated model of ischemic injury, there was very little delayed apoptotic cell death. This is uncharacteristic compared to other models of focal ischemia, where cell death is mostly necrotic at the time of insult, followed by a secondary cell death phase that is mostly apoptotic (Sairanen, Karjalainen-Lindsberg, Paetau, Ijäs, & Lindsberg, 2006). Necrotic cell death was not assessed in this study, and an examination of apoptotic cell death revealed some active caspase 3 staining at 1 day post-stroke which declined by 3 days post-stroke. Apoptotic cell death was no longer observed at 7 and 10 days post-stroke. This was in contrast to the saline injuries where no active caspase 3 labeling was observed, only a few apoptotic nuclei. Apoptotic cell death following ischemia is associated with the delayed excitotoxic response to excess extracellular glutamate which occurs between 0-24 hours post ischemia (Dávalos, Castillo, Serena, & Noya, 1997). The apoptotic process takes approximately 6-24 hours (Saraste & Pulkki, 2000) and since apoptotic cells are positive for active caspase-3 for a period of approximately 4 hours, it is highly likely that some apoptotic cells were missed between 1 and 3 days post ischemia.

Although the results show a trend towards smaller injury volumes from 1 to 10 days post-stroke, significant cell death was not observed beyond 3 days suggesting that changes in injury volume cannot be attributed to apoptotic cell death. Thus, the lack of apoptosis at 7

and 10 days post-stroke and the low level of edema following a small ET-1 injury results in a relatively stable sized injury within one week post-stroke. This is in contrast to the larger changes in the stroke volume observed in larger injuries such as MCAo.

4.1.2 Glial cell activation is spatially and temporally defined by different cell types.

In this study, the responses of glial cells were assessed to both ET-1 injections and saline injections. Activated astrocytes were observed in both ET-1 and saline conditions, however a greater level of activated astrocytes were observed further from the site of injury in ET-1 conditions. While studying the immune cell response to both ET-1 and saline injuries, robust activated immune responses were not observed until 3 days post-injury. When activated immune cells were observed, they were confined to the site of injury and any separation of resident microglia and infiltrating macrophages was not possible using the immunohistochemical markers available. However when the two types of injuries were compared a greater area of activated immune cells was observed in ET-1 mediated injuries. The differences in the quality of the glial cells responses between ET-1 and saline injuries are further proof to the validity of the ET-1 injection model of focal ischemia.

4.1.2.1 Astrocyte activation spreads across the cortex.

Following an ET-1 stroke, astrocyte activation spreads across the injured cortex. This has been characterized over the first 10 days through the following observations. Immediately following a stroke, astrocytes become activated surrounding the injury. By 3 days post-stroke, astrocyte activation has spread across the ipsilateral cortex and by 7 days it has

spread into the contralateral cortex. While the upregulation of GFAP expression as an indicator of astrocyte activation did not differ between cells that were at the border of the injury, the presence of activated cells further from the site of injury was significantly greater by 7 days post-stroke. Astrocytes are commonly activated following ischemic injuries (Gladstone et al., 2002). In MCAo injuries, astrocytes are activated as early as 4 hours post-stroke and begin to decrease by 14 days post-stroke (Barreto et al., 2012; Sofroniew, 2009; Stoll, 1998). Despite a decrease in the levels of astrocyte activation over time, astrocytes surrounding the injury site remain activated in larger models of ischemic injury (Sofroniew, 2009; Stoll, 1998). Following MCAo, astrocyte activation as assessed by GFAP upregulation is seen throughout the ipsilateral cortex beginning at 4 hours post-stroke, continuing until 7 days post-stroke, and persisting around the border of the injury up to 60 days post-stroke (Nowicka, Rogozinska, Aleksy, Witte, & Skangiel-Kramska, 2008). Robust levels of astrocyte activation were also found in the peri-infarct area in photothrombosis (Kuraoka et al., 2009; Nowicka et al., 2008). This persistent activation of astrocytes was observed in this study along the border of the injury as demonstrated at 10 days post ET-1 induced stroke. Astrocytes remain activated near the border of the injury. Until the current study, the spread of astrocyte activation into the contralateral cortex has not previously been reported. Although an ET-1 ischemic infarct is significantly smaller than an MCAo or photothrombotic infarct, we observed extensive activation of astrocytes across the ipsilateral cortex and into the contralateral cortex. To the best of my knowledge, the spreading of astrocyte activation was observed for the first time in this thesis. As this study only examined the first 10 days post-stroke, it is unclear the duration of astrocyte activation or whether it would be comparable in a human stroke

brain. One potential mechanism to mediate the spread of astrocyte activation is cell to cell communication through gap junctions (Huang et al., 2012). Further studies into identifying the mechanism that mediates the spread of astrocyte activation and what role it plays in the contralateral cortex is important to understand the full impact these cells can have in stroke recovery.

The contrasting roles of activated astrocytes, having both pro and anti-inflammatory effects, give them a complex role in the post-stroke cortex. Activated astrocytes play a pro-survival role by secreting factors that aid neuronal survival. These factors include adenosine triphosphate (ATP), glutamate and D-serine in quantities that can promote cell survival in a controlled manner (Deb et al., 2010; Guthrie et al., 1999). This is in addition to neurotrophic factors like BDNF, NGF and heat shock proteins (Hsps) (do Carmo Cunha et al., 2007; White, Yin, & Jakeman, 2008). Post-stroke there is a large uncontrolled release of glutamate from dead and dying cells (Brassai, Suvanjeiev, Bán, & Lakatos, 2015). One of the pro-survival functions of astrocytes post-stroke, is the ability to uptake this potentially cytotoxic glutamate (Sofroniew, 2009; Takatsuru et al., 2013). However, astrocytes also produce ROS, which can induce apoptosis, and result in the release of excess glutamate (Deb et al., 2010; Sofroniew, 2009; Stoll, 1998). If glutamate is released in high concentrations, it is excitotoxic to neurons. Astrocytes play a protective role by uptaking excess toxic glutamate and metabolizing it into the non-toxic neurotransmitter precursor glutamine (Takatsuru et al., 2013). Astrocytes therefore, have a direct impact on the survival of surrounding cells. Therefore, it is important to understand where and when astrocytes are activated in the cortex post-stroke. In the

future, strategies may be able to target their activation to promote the survival of cells post-stroke.

4.1.2.2 Microglia and macrophages show a delayed reaction to an ischemic injury.

Following either a saline or ET-1 injection, activated immune cells, as demonstrated by α-CD-68 immunohistochemistry were first observed at 3 days post-surgery in this study. Few to no cells were observed at 1 day, except along the needle tract. Although the 2 day time point was not assessed, by 3 days post-surgery widespread CD-68 positive cells were observed throughout the injury sites. By 10 days post-stroke, the number of activated immune cells had decreased with cells centered once again around the needle tracts. A larger area of α-CD-68 positive cells was found following an ET-1 injury consistent with larger injury volumes in stroke injuries versus saline injuries. However, no significant differences were detected in the density of activated immune cells within the injuries at any time point. While the area covered by activated immune cells does change over the first 10 days post-stroke, the level of activation, as measured by the amount of CD-68 did not change. Furthermore the level of CD-68 upregulation can be attributed to the damage caused by the injury because both saline and ET-1 induced injuries resulted in a similar level of CD-68 upregulation. One of the potential reasons for the area of activated immune cells remaining elevated by 7 days post-surgery can be a breakdown of the blood brain barrier which would allow infiltrating macrophages to enter the injury (Brouns & De Deyn, 2009). However, it is not uncommon for activated immune cells to be detected from as early as 6 hours through to 21 days following MCAo

(Lehrmann et al., 1997; Nowicka et al., 2008; Walberer et al., 2010). This suggests that larger injuries may recruit more peripheral macrophages. It is important to note that while immune cell activation following MCAo and photothrombosis is larger than what is seen in ET-1 mediated ischemic injuries, immune cell activation is confined to the infarct core in all ischemic models (Lehrmann et al., 1997; Nowicka et al., 2008; Taylor & Sansing, 2013). Post-mortem studies in human tissue have reported immune cell activation early at 24 hours post-stroke and higher levels at 72 hours post-stroke through the use of Iba-1 and radiolabeling for activated microglia (Price et al., 2006; Taylor & Sansing, 2013). These findings are in contrast to my results where little to no immune cell activation was observed at 1 day post-stroke with anti-CD-68 immunohistochemistry. Although not examined in this study, assessing immune cell activation at 2 days following an ET-1 stroke may have demonstrated when cells are activated following injury. However, extensive immune cell activation was observed within the injury site by 3 days post-surgery consistent with other stroke models. The reduction in the area occupied by activated immune cells by 10 days post-stroke, suggests that the immune response is beginning to resolve. In contrast, current models of focal ischemia, such as MCAo create larger injuries that recruit a large immune response which often don't become quiescent up to 60 days post-stroke (Nowicka et al., 2008). Therefore, the significantly smaller injury observed in an ET-1 meditated ischemic injury creates a smaller immune response than that observed following MCAo. Small injuries in which the immune cell activation become resolved faster than in large injuries will be valuable to assess the progression of the immune response post-stroke and its importance in promoting neural repair.

4.1.3 The newborn neuroblast cells are significantly increased within the SVZ over the 10 days post-stroke.

Following either saline or ET-1 injections, no significant change in cell proliferation was observed within the SVZ over the first 10 days post-stroke. This is in contrast to the proliferative response seen in MCAo and photothrombosis models of ischemic injury. In these models there is a significant increase in the proliferating population from 1 week up to one year post-stroke (Osman et al., 2011; Thored et al., 2006). Previous studies have shown that the size of an injury is positively correlated with the proliferative response from NPCs (Thored et al., 2006). In this study, while there was robust positive staining there was no significant change seen between ischemic conditions and saline controls. Therefore, the proliferative response from a small focal ischemic injury, such as the one in this study, may be too small to be detected using the current BrdU labeling protocol. Other potential explanations for the lack of detection of a NPC response in this study may be attributed to the characteristics of BrdU and the protocol employed in this study. BrdU only labels cells during S-phase of the cell cycle and has a half-life *in vivo* of 2 hours. In this study, mice received IP injections on the day of euthanasia every 2 hours over a 6.5hr period, therefore only cells in S-phase during this 6.5 hour window would be labeled with BrdU. The goal of the labeling protocol used in the study was to identify the time point following stroke when NPCs within the SVZ respond by increasing proliferation. Proliferating NPCs were only quantified in the ipsilateral hemisphere and comparisons were made between ET-1 and saline injected brains. Due to the small size of the ET-1 induced infarct and the damage associated with a saline injection there were no

significant differences in the number of proliferating cells. Although comparisons were not made between ET-1, saline and naïve any differences in proliferation above that of naïve would be attributed to the damage associated with the cortical injections.

Different markers of cell proliferation may provide a different picture. For instance, Ki67 is a protein that is upregulated during all phases of the cell cycle (Abeysinghe, Bokhari, Dusting, & Roulston, 2014). Ki67 immunohistochemistry therefore labels all cells that are proliferating at the time of sacrifice. In contrast, BrdU labels cells in S-phase of the cell cycle. Therefore the trade-off is labeling all proliferating cells at a specific time point, or identifying the cells that are actively dividing over a two hour time period. Alternatively BrdU can be applied over a longer time course, to capture a larger proportion of the proliferative population (Arvidsson et al., 2002). Although this would capture more global changes in the proliferative state of cells, it lacks the precision of the shorter time window. The lack of precision is because it is impossible to determine when the cell was labeled during a given BrdU pulse, only that the cell had undergone mitosis during the pulse. This is one of the reasons why this study has a focal approach to BrdU administration that occurs during one period, therefore all BrdU positive cells had undergone mitosis on the day of sacrifice.

One goal of understanding the NPC response post-stroke is to selectively study neuroblasts, the NPC population that responds to a stroke by differentiating. This thesis shows there is a significant increase in the newborn neuroblast population that responds to a small focal ischemic injury, and peaks at 7 days post-stroke. This subset of the NPC population can leave the SVZ and migrate towards the site of injury (Doetsch, 2003;

Ohab, Fleming, Blesch, & Carmichael, 2006). The peak of the newborn neuroblast response corresponds to similar time points in other models, such as MCAo and photothrombosis, where the maximum number of migrating neuroblasts are observed at 1 and 2 weeks post stroke (Osman et al., 2011; Thored et al., 2006). However, these models show a more robust response than observed in the current ET-1 mediated small focal injury, likely because larger injuries induce a larger NPC response (Abeysinghe et al., 2014). Unfortunately, few studies assess the NPC response within the first week post-stroke (A. Arvidsson et al., 2002; Osman et al., 2011; Parent et al., 2002; Thored et al., 2006). There is a lack of knowledge of how soon the NPC response is initiated post-stroke. In the current study, the NPC response was examined at 1, 3, 7 and 10 days post-stroke. We found an increase in newborn neuroblasts at 7 days which was diminished 3 days later. There are a few possible reasons for the decrease observed. One is that the increase is a transient response and by 10 days post-stroke these neuroblasts may have differentiated into mature cell types or do not survive. Additionally, NPCs could have migrated from the SVZ either along the rostral migratory stream or into the cortex while quantification was confined to the SVZ. Another question is why there was a response in the newborn neuroblasts with no significant increase in the NPC population observed. A possible explanation is that the change in the newborn neuroblast population is not large enough to significantly affect the levels of the total proliferative population of the SVZ. This could occur because the majority of the proliferative population remains in a state of self-proliferation as opposed to differentiation into neuroblasts (Thored et al., 2006). In conclusion, this thesis has shown that the total NPC population does not change its

proliferative state at any specific time point over the first 10 days post-stroke, but it does have an increase of the newborn neuroblast population at 7 days.

4.2 Future Directions

This thesis focused on the characterization of a small focal ischemic injury and has led to a number of interesting questions. These questions can be classified into two groups. The first focuses on the glial responses post-stroke, and the second involves understanding the NPC responses in the hope to improve their survival post-stroke. The focus on the glial responses includes identifying the mechanism of the spread seen in astrocyte activation and the role astrocytes play in the cortex outside of the peri-infarct area post-stroke. This is in conjunction with assessing the immune response to an ischemic injury. This includes how immune cells infiltrate and when breakdown of the blood brain barrier occurs in this model of ischemic injury. The second group of questions, focusing on the NPC responses, would be trying to target the differentiating population of NPCs post-stroke, when this differentiation occurs and how the migratory neuroblasts can be targeted to improve their survival in the ischemic cortex. Overall, these future directions can build upon the findings in this thesis in the hope of improving stroke recovery.

The first direction is to follow the glial cell responses post-stroke. Specifically, the first experiment would be identifying the potential mechanism behind the spread of astrocyte activation across the ischemic cortex and into the contralateral hemisphere post-stroke. Another potential experiment would be to assess the role of gap junctions in activating astrocytes post-stroke. Gap junctions have the ability to directly mediate communications between cells by forming physical connections between the cells. There has been research

into the role gap junctions play in mediating neuroprotection post-stroke, and the subunits that compose gap junctions (Kozoriz et al., 2010). Specifically assessing the role of gap junctions in affecting the spread of astrocyte activation may be observed through the transfer of a gap junction permeable dye such as calcein-AM. This method would assess the activity of gap junctions as a method to transport potential signalling molecules between astrocytes (Roemer, Lammerich, Conroy, & Weisensee, 2013). If gap junctions are the source of the spread of astrocyte activation post-stroke, then modifying gap junctions could confine where astrocytes are activated post-stroke.

The second part of the glial response studied was the immune cell response to a small focal ischemic injury. Future directions from this study include understanding why there is a delay in the response of the immune cells to an injury. Is this delay consistent with a breakdown of the BBB, and when does this breakdown occur? Breakdown of the BBB allows macrophages to infiltrate into the brain (Kawano et al., 2012; Walberer et al., 2010). This could lead to selectively studying the response of microglia as the only immune cells responding to an injury prior to the breakdown of the BBB. Additionally, the role that these immune cells play in the brain can be further investigated by assessing immune cell polarization as either cytotoxic M1 or neurotrophic M2 phenotypes (Benarroch, 2013; Taylor & Sansing, 2013). If there is a switch between M1 and M2 phenotypes, determining when this switch occurs and if there is a method to promote the M2 phenotype could provide a therapy to promote recovery post-stroke.

The second group of future directions involves studying the NPC responses post-stroke. In this thesis, there has been a specific increase in the newborn neuroblast response at 7

days post-stroke. The goal of tracking neuroblasts from the SVZ towards the site of injury and determining their fate once they arrive is still very much a possibility with different techniques. Techniques such as labelling NPCs through viral transfection or electroporation would allow for more robust tracking. If robust tracking is possible then targeting these NPCs with genetic based therapies would allow for temporal control of novel therapies *in vivo*. One method to improve tracking, and then introduce genetic therapies into NPCs is through *in vivo* electroporation or virus infection of a plasmid containing a fluorescent reporter or a potentially therapeutic gene. Introducing a pro-survival gene via these methods could produce new mature neurons into the injured brain and potentially improve stroke recovery. If these NPCs, including differentiating neuroblasts, can migrate to the site of injury and survive they can play two major roles in promoting repair (Burns & Steinberg, 2011). The first is their ability to differentiate into mature neurons that can help replace some of the lost neurons. The second major role these NPCs can play is to provide support to the surviving cells at the site of injury (Ohab et al., 2006). It is important to be able to leverage their abilities to become mature functioning neurons in the brain post-stroke.

4.3 Conclusion

This thesis has characterized the endogenous responses following a small focal ischemic injury. This has included identifying a stable sized injury following ET-1 mediated ischemic injury, with apoptotic cell death up to 3 days post-stroke. The responses of glial cells were studied with both activated astrocytes and immune cells being quantified up to 10 days post-stroke. This showed for the first time a spread of astrocyte activation into

the contralateral cortex to the ischemic injury. This is an exciting observation that shows how astrocytes play a larger role across areas that have previously been assumed to be healthy and minimally affected by a small ischemic injury. Additionally, the NPC and newborn neuroblast populations were quantified over the first 10 days post-stroke and a peak level of newborn neuroblasts was identified at 7 days post-ischemic injury. This can potentially be used as a target for impacting the highest number of newborn neuroblasts to improve survival and have an impact on stroke recovery.

Bibliography

Aberg, M. a, Aberg, N. D., Hedbäcker, H., Oscarsson, J., & Eriksson, P. S. (2000). Peripheral infusion of IGF-I selectively induces neurogenesis in the adult rat hippocampus. *The Journal of Neuroscience : The Official Journal of the Society for Neuroscience*, *20*(8), 2896–2903.

Abeysinghe, H. C. S., Bokhari, L., Dusting, G. J., & Roulston, C. L. (2014). Brain remodelling following endothelin-1 induced stroke in conscious rats. *PloS One*, *9*(5), e97007. doi:10.1371/journal.pone.0097007

Adamson, J., Beswick, A., & Ebrahim, S. (2004). Is stroke the most common cause of disability? *Journal of Stroke and Cerebrovascular Diseases : The Official Journal of National Stroke Association*, *13*(4), 171–7. doi:10.1016/j.jstrokecerebrovasdis.2004.06.003

Adkins-Muir, D. L., & Jones, T. A. (2003). Cortical electrical stimulation combined with rehabilitative training: enhanced functional recovery and dendritic plasticity following focal cortical ischemia in rats. *Neurological Research*, *25*(8), 780–8. doi:10.1179/016164103771953853

Albers, G. W., Thijs, V. N., Wechsler, L., Kemp, S., Schlaug, G., Skalabrin, E., … Marks, M. P. (2006). Magnetic resonance imaging profiles predict clinical response to early reperfusion: the diffusion and perfusion imaging evaluation for understanding stroke evolution (DEFUSE) study. *Annals of Neurology*, *60*(5), 508–17. doi:10.1002/ana.20976

Aldskogius, H., & Kozlova, E. N. (1998). Central neuron-glial and glial-glial interactions following axon injury. *Progress in Neurobiology*, *55*(1), 1–26. Retrieved from http://www.ncbi.nlm.nih.gov/pubmed/9602498

Andersen, K. K., Olsen, T. S., Dehlendorff, C., & Kammersgaard, L. P. (2009). Hemorrhagic and ischemic strokes compared: stroke severity, mortality, and risk factors. *Stroke; a Journal of Cerebral Circulation*, *40*(6), 2068–72. doi:10.1161/STROKEAHA.108.540112

Arvidsson, a., Kokaia, Z., Airaksinen, M. S., Saarma, M., & Lindvall, O. (2001). Stroke induces widespread changes of gene expression for glial cell line-derived neurotrophic factor family receptors in the adult rat brain. *Neuroscience*, *106*(1), 27–41. doi:10.1016/S0306-4522(01)00268-8

Arvidsson, A., Collin, T., Kirik, D., Kokaia, Z., & Lindvall, O. (2002). Neuronal replacement from endogenous precursors in the adult brain after stroke. *Nature Medicine*. doi:10.1038/nm

Astrup, J., Siesjo, B. K., & Symon, L. (1981). Thresholds in cerebral ischemia - the ischemic penumbra. *Stroke*, *12*(6), 723–725. doi:10.1161/01.STR.12.6.723

Banerjee, S., Williamson, D. a, Habib, N., & Chataway, J. (2012). The potential benefit of stem cell therapy after stroke: an update. *Vascular Health and Risk Management*, *8*, 569–80. doi:10.2147/VHRM.S25745

Barber, P. A., Zhang, J., Demchuk, A. M., Hill, M. D., & Buchan, A. M. (2001). Why are stroke patients excluded from TPA therapy?: An analysis of patient eligibility. *Neurology*, *56*(8), 1015–1020. doi:10.1212/WNL.56.8.1015

Baron, J.-C., Yamauchi, H., Fujioka, M., & Endres, M. (2014). Selective neuronal loss in ischemic stroke and cerebrovascular disease. *Journal of Cerebral Blood Flow and Metabolism : Official Journal of the International Society of Cerebral Blood Flow and Metabolism*, *34*(1), 2–18. doi:10.1038/jcbfm.2013.188

Barreto, G. E., White, R. E., Xu, L., Palm, C. J., & Giffard, R. G. (2012). Effects of heat shock protein 72 (Hsp72) on evolution of astrocyte activation following stroke in the mouse. *Experimental Neurology*, *238*(2), 284–96. doi:10.1016/j.expneurol.2012.08.015

Becker, K. J. (1998). Inflammation and acute stroke. *Current Opinion in Neurology*, *11*(1), 45–9. Retrieved from http://www.ncbi.nlm.nih.gov/pubmed/9484616

Belayev, L., Khoutorova, L., Zhao, W., Vigdorchik, A., Belayev, A., Busto, R., … Ginsberg, M. D. (2005). Neuroprotective effect of darbepoetin alfa, a novel recombinant erythropoietic protein, in focal cerebral ischemia in rats. *Stroke*, *36*, 1065–1070. doi:10.1161/01.STR.0000160753.36093.da

Benarroch, E. E. (2013). Microglia: Multiple roles in surveillance, circuit shaping, and response to injury. *Neurology*, *81*(12), 1079–88. doi:10.1212/WNL.0b013e3182a4a577

Benowitz, L. I., & Carmichael, S. T. (2010). Promoting axonal rewiring to improve outcome after stroke. *Neurobiology of Disease*, *37*(2), 259–66. doi:10.1016/j.nbd.2009.11.009

Biernaskie, J., Chernenko, G., & Corbett, D. (2004). Efficacy of rehabilitative experience declines with time after focal ischemic brain injury. *The Journal of Neuroscience :*

The Official Journal of the Society for Neuroscience, *24*(5), 1245–54. doi:10.1523/JNEUROSCI.3834-03.2004

Brassai, a., Suvanjeiev, R.-G., Bán, E.-G., & Lakatos, M. (2015). Role of synaptic and nonsynaptic glutamate receptors in ischaemia induced neurotoxicity. *Brain Research Bulletin*, *112*, 1–6. doi:10.1016/j.brainresbull.2014.12.007

Bronnum-Hansen, H., Davidsen, M., & Thorvaldsen, P. (2001). Long-Term Survival and Causes of Death After Stroke. *Stroke*, *32*(9), 2131–2136. doi:10.1161/hs0901.094253

Brouns, R., & De Deyn, P. P. (2009). The complexity of neurobiological processes in acute ischemic stroke. *Clinical Neurology and Neurosurgery*, *111*(6), 483–95. doi:10.1016/j.clineuro.2009.04.001

Burns, T. C., & Steinberg, G. K. (2011). Stem cells and stroke: opportunities, challenges and strategies. *Expert Opinion on Biological Therapy*, *11*(4), 447–61. doi:10.1517/14712598.2011.552883

Bush, T., Puvanachandra, N., Horner, C., Polito, A., Ostenfeld, T., Svendsen, C., … Sofroniew, M. (1999). Leukocyte Infiltration, Neuronal Degeneration, and Neurite Outgrowth after Ablation of Scar-Forming, Reactive Astrocytes in Adult Transgenic Mice. *Neuron*, *23*(2), 297–308. doi:10.1016/S0896-6273(00)80781-3

Carmichael, S. T. (2005). Rodent models of focal stroke: size, mechanism, and purpose. *NeuroRx : The Journal of the American Society for Experimental NeuroTherapeutics*, *2*(3), 396–409. doi:10.1602/neurorx.2.3.396

Carmichael, S. T., Archibeque, I., Luke, L., Nolan, T., Momiy, J., & Li, S. (2005). Growth-associated gene expression after stroke: evidence for a growth-promoting region in peri-infarct cortex. *Experimental Neurology*, *193*(2), 291–311. doi:10.1016/j.expneurol.2005.01.004

Chen, Y., Samal, B., Hamelink, C. R., Xiang, C. C., Chen, Y., Chen, M., … Eiden, L. E. (2006). Neuroprotection by endogenous and exogenous PACAP following stroke. *Regulatory Peptides*, *137*, 4–19. doi:10.1016/j.regpep.2006.06.016

Christie, K. J., & Turnley, A. M. (2012). Regulation of endogenous neural stem/progenitor cells for neural repair-factors that promote neurogenesis and gliogenesis in the normal and damaged brain. *Frontiers in Cellular Neuroscience*, *6*(January), 70. doi:10.3389/fncel.2012.00070

Clarkson, A. N., López-Valdés, H. E., Overman, J. J., Charles, A. C., Brennan, K. C., & Thomas Carmichael, S. (2013). Multimodal examination of structural and functional

remapping in the mouse photothrombotic stroke model. *Journal of Cerebral Blood Flow and Metabolism : Official Journal of the International Society of Cerebral Blood Flow and Metabolism*, *33*(5), 716–23. doi:10.1038/jcbfm.2013.7

Dávalos, A., Castillo, J., Serena, J., & Noya, M. (1997). Duration of Glutamate Release After Acute Ischemic Stroke. *Stroke* , *28* (4), 708–710. doi:10.1161/01.STR.28.4.708

Deb, P., Sharma, S., & Hassan, K. M. (2010). Pathophysiologic mechanisms of acute ischemic stroke : An overview with emphasis on therapeutic significance beyond thrombolysis. *Pathophysiology*, *17*(3), 197–218. doi:10.1016/j.pathophys.2009.12.001

Del Zoppo, G. J., Saver, J. L., Jauch, E. C., & Adams, H. P. (2009). Expansion of the time window for treatment of acute ischemic stroke with intravenous tissue plasminogen activator: a science advisory from the American Heart Association/American Stroke Association. *Stroke; a Journal of Cerebral Circulation*, *40*(8), 2945–8. doi:10.1161/STROKEAHA.109.192535

Dereski, M., Chopp, M., Knight, R., Rodolosi, L., & Garcia, J. (1993). The heterogeneous temporal evolution of focal ischemic neuronal damage in the rat. *Acta Neuropathologica*, *85*(3). doi:10.1007/BF00227730

Do Carmo Cunha, J., de Freitas Azevedo Levy, B., de Luca, B. A., de Andrade, M. S. R., Gomide, V. C., & Chadi, G. (2007). Responses of reactive astrocytes containing S100beta protein and fibroblast growth factor-2 in the border and in the adjacent preserved tissue after a contusion injury of the spinal cord in rats: implications for wound repair and neuroregeneration. *Wound Repair and Regeneration : Official Publication of the Wound Healing Society [and] the European Tissue Repair Society*, *15*(1), 134–46. doi:10.1111/j.1524-475X.2006.00194.x

Doeppner, T. R., El Aanbouri, M., Dietz, G. P. H., Weise, J., Schwarting, S., & Bähr, M. (2010). Transplantation of TAT-Bcl-xL-transduced neural precursor cells: long-term neuroprotection after stroke. *Neurobiology of Disease*, *40*(1), 265–76. doi:10.1016/j.nbd.2010.05.033

Doetsch, F. (2003). A niche for adult neural stem cells. *Current Opinion in Genetics & Development*, *13*(5), 543–550. doi:10.1016/j.gde.2003.08.012

Falcao, A. L. E., Reutens, D. C., Markus, R., Koga, M., Read, S. J., Tochon-Danguy, H., … Donnan, G. a. (2004). The resistance to ischemia of white and gray matter after stroke. *Annals of Neurology*, *56*(5), 695–701. doi:10.1002/ana.20265

Fang, M. C., Perraillon, M. C., Ghosh, K., Cutler, D. M., & Rosen, A. B. (2014). Trends in Stroke Rates, Risk, and Outcomes in the United States, 1988-2008. *The American Journal of Medicine*. doi:10.1016/j.amjmed.2014.03.017

Fischer, U., Arnold, M., Nedeltchev, K., Schoenenberger, R. A., Kappeler, L., Höllinger, P., … Mattle, H. P. (2006). Impact of comorbidity on ischemic stroke outcome. *Acta Neurologica Scandinavica*, *113*(2), 108–13. doi:10.1111/j.1600-0404.2005.00551.x

Fisher, M., Feuerstein, G., Howells, D. W., Hurn, P. D., Kent, T. a, Savitz, S. I., & Lo, E. H. (2009). Update of the stroke therapy academic industry roundtable preclinical recommendations. *Stroke; a Journal of Cerebral Circulation*, *40*(6), 2244–50. doi:10.1161/STROKEAHA.108.541128

Fonarow, G. C., Zhao, X., Smith, E. E., Saver, J. L., Reeves, M. J., Bhatt, D. L., … Schwamm, L. H. (2014). Door-to-needle times for tissue plasminogen activator administration and clinical outcomes in acute ischemic stroke before and after a quality improvement initiative. *JAMA : The Journal of the American Medical Association*, *311*(16), 1632–40. doi:10.1001/jama.2014.3203

Fuxe, K., Bjelke, B., Andbjer, B., Grahn, H., Rimondini, R., & Agnati, L. F. (1997). Endothelin-1 induced lesions of the frontoparietal cortex of the rat. A possible model of focal cortical ischemia. *Neuroreport*, *8*(11), 2623–9. Retrieved from http://www.ncbi.nlm.nih.gov/pubmed/9261839

Gage, F. H., Ray, J., & Fisher, L. J. (1995). Isolation, characterization, and use of stem cells from the CNS. *Annual Review of Neuroscience*, *18*, 159–92. doi:10.1146/annurev.ne.18.030195.001111

Garcia, J. H., Yoshida, Y., Chen, H., Li, Y., Zhang, Z. G., Lian, J., … Chopp, M. (1993). Progression from ischemic injury to infarct following middle cerebral artery occlusion in the rat. *The American Journal of Pathology*, *142*(2), 623–35. Retrieved from http://www.pubmedcentral.nih.gov/articlerender.fcgi?artid=1886726&tool=pmcentrez&rendertype=abstract

Gladstone, D. J., Black, S. E., & Hakim, a. M. (2002). Toward Wisdom From Failure: Lessons From Neuroprotective Stroke Trials and New Therapeutic Directions. *Stroke*, *33*(8), 2123–2136. doi:10.1161/01.STR.0000025518.34157.51

Gleeson, J. G., Peter T, L., Flanagan, L. A., & Walsh, C. A. (1999). Doublecortin is a microtubule-associated protein and is expressed widely by migrating neurons. *Neuron*, *23*(2), 257–271.

Guillemin, G. J., & Brew, B. J. (2004). Microglia, macrophages, perivascular macrophages, and pericytes: a review of function and identification. *Journal of Leukocyte Biology*, *75*(3), 388–97. doi:10.1189/jlb.0303114

Guthrie, P. B., Knappenberger, J., Segal, M., Bennett, M. V. L., Charles, A. C., & Kater, S. B. (1999). ATP Released from Astrocytes Mediates Glial Calcium Waves, *19*(2), 520–528.

Hall, a P., Davies, W., Stamp, K., Clamp, I., & Bigley, A. (2013). Comparison of Computerized Image Analysis with Traditional Semiquantitative Scoring of Perls' Prussian Blue Stained Hepatic Iron Deposition. *Toxicologic Pathology*. doi:10.1177/0192623313476576

Harrison, T. C., & Murphy, T. H. (2012). Towards a circuit mechanism for movement tuning in motor cortex. *Frontiers in Neural Circuits*, *6*, 127. doi:10.3389/fncir.2012.00127

Hicks, A. U., MacLellan, C. L., Chernenko, G. A., & Corbett, D. (2008). Long-term assessment of enriched housing and subventricular zone derived cell transplantation after focal ischemia in rats. *Brain Research*, *1231*, 103–12. doi:10.1016/j.brainres.2008.07.041

Hinkle, J. L., & Guanci, M. M. (2007). Acute Ischemic Stroke Review Pathophysiology, *39*(5), 285–293.

Hodgson, C. (1998). Emergency management of acute ischemic stroke in Canadian hospitals, *159*, 15–18.

Horie, N., Maag, A.-L., Hamilton, S. A., Shichinohe, H., Bliss, T. M., & Steinberg, G. K. (2008). Mouse model of focal cerebral ischemia using endothelin-1. *Journal of Neuroscience Methods*, *173*(2), 286–90. doi:10.1016/j.jneumeth.2008.06.013

Horn, S. D., DeJong, G., Smout, R. J., Gassaway, J., James, R., & Conroy, B. (2005). Stroke rehabilitation patients, practice, and outcomes: is earlier and more aggressive therapy better? *Archives of Physical Medicine and Rehabilitation*, *86*(12 Suppl 2), S101–S114. doi:10.1016/j.apmr.2005.09.016

Hou, S. W., Wang, Y. Q., Xu, M., Shen, D. H., Wang, J. J., Huang, F., … Sun, F. Y. (2008). Functional integration of newly generated neurons into striatum after cerebral ischemia in the adult rat brain. *Stroke*, *39*, 2837–2844. doi:10.1161/STROKEAHA.107.510982

Huang, C., Han, X., Li, X., Lam, E., Peng, W., Lou, N., … Takano, T. (2012). Critical role of connexin 43 in secondary expansion of traumatic spinal cord injury. *The*

Journal of Neuroscience : The Official Journal of the Society for Neuroscience, *32*(10), 3333–8. doi:10.1523/JNEUROSCI.1216-11.2012

Huang, L., Wu, Z.-B., Zhuge, Q., Zheng, W., Shao, B., Wang, B., … Jin, K. (2014). Glial scar formation occurs in the human brain after ischemic stroke. *International Journal of Medical Sciences*, *11*(4), 344–8. doi:10.7150/ijms.8140

Hughes, P. M., Anthony, D. C., Ruddin, M., Botham, M. S., Rankine, E. L., Sablone, M., … Perry, V. H. (2003). Focal lesions in the rat central nervous system induced by endothelin-1. *Journal of Neuropathology and Experimental Neurology*, *62*(12), 1276–86. Retrieved from http://www.ncbi.nlm.nih.gov/pubmed/14692703

Iadecola, C., & Anrather, J. (2011). The immunology of stroke: from mechanisms to translation. *Nature Medicine*, *17*(7), 796–808. doi:10.1038/nm.2399

Im, S. H., Yu, J. H., Park, E. S., Lee, J. E., Kim, H. O., Park, K. I., … Cho, S. R. (2010). Induction of striatal neurogenesis enhances functional recovery in an adult animal model of neonatal hypoxic-ischemic brain injury. *Neuroscience*, *169*(1), 259–268. doi:10.1016/j.neuroscience.2010.04.038

Jin, K., Wang, X., Xie, L., Mao, X. O., & Greenberg, D. a. (2010). Transgenic ablation of doublecortin-expressing cells suppresses adult neurogenesis and worsens stroke outcome in mice. *Proceedings of the National Academy of Sciences of the United States of America*, *107*(17), 7993–8. doi:10.1073/pnas.1000154107

Kahle, M. P., & Bix, G. J. (2013). Neuronal restoration following ischemic stroke: influences, barriers, and therapeutic potential. *Neurorehabilitation and Neural Repair*, *27*(5), 469–78. doi:10.1177/1545968312474119

Kasner, S. E., Demchuk, a M., Berrouschot, J., Schmutzhard, E., Harms, L., Verro, P., … Krieger, D. W. (2001). Predictors of fatal brain edema in massive hemispheric ischemic stroke. *Stroke; a Journal of Cerebral Circulation*, *32*(9), 2117–23. Retrieved from http://www.ncbi.nlm.nih.gov/pubmed/11546905

Kawano, H., Kimura-Kuroda, J., Komuta, Y., Yoshioka, N., Li, H. P., Kawamura, K., … Raisman, G. (2012). Role of the lesion scar in the response to damage and repair of the central nervous system. *Cell and Tissue Research*, *349*(1), 169–80. doi:10.1007/s00441-012-1336-5

Kobayashi, T., Ahlenius, H., Thored, P., Kobayashi, R., Kokaia, Z., & Lindvall, O. (2006). Intracerebral infusion of glial cell line-derived neurotrophic factor promotes striatal neurogenesis after stroke in adult rats. *Stroke*, *37*, 2361–2367. doi:10.1161/01.STR.0000236025.44089.e1

Kokaia, Z., Thored, P., Arvidsson, A., & Lindvall, O. (2006). Regulation of stroke-induced neurogenesis in adult brain--recent scientific progress. *Cerebral Cortex (New York, N.Y. : 1991)*, *16 Suppl 1*, i162–7. doi:10.1093/cercor/bhj174

Kornblum, H. I. (2007). Introduction to neural stem cells. *Stroke; a Journal of Cerebral Circulation*, *38*(2 Suppl), 810–6. doi:10.1161/01.STR.0000255757.12198.0f

Kozoriz, M. G., Bechberger, J. F., Bechberger, G. R., Suen, M. W. H., Moreno, A. P., Maass, K., … Naus, C. C. (2010). The connexin43 C-terminal region mediates neuroprotection during stroke. *Journal of Neuropathology and Experimental Neurology*, *69*(2), 196–206. doi:10.1097/NEN.0b013e3181cd44df

Krakauer, J. W., Carmichael, S. T., Corbett, D., & Wittenberg, G. F. (2012). Getting neurorehabilitation right: what can be learned from animal models? *Neurorehabilitation and Neural Repair*, *26*(8), 923–31. doi:10.1177/1545968312440745

Kuhn, H. G., Winkler, J., Kempermann, G., Thal, L. J., & Gage, F. H. (1997). Epidermal growth factor and fibroblast growth factor-2 have different effects on neural progenitors in the adult rat brain. *The Journal of Neuroscience : The Official Journal of the Society for Neuroscience*, *17*(15), 5820–9. Retrieved from http://www.ncbi.nlm.nih.gov/pubmed/9221780

Kuraoka, M., Furuta, T., Matsuwaki, T., & Omatsu, T. (2009). Direct Experimental Occlusion of the Distal Middle Cerebral Artery Induces High Reproducibility of Brain Ischemia in Mice, *58*(April 2008), 19–29.

Kwakkel, G. (2006). Impact of intensity of practice after stroke: issues for consideration. *Disability and Rehabilitation*, *28*(13-14), 823–30. doi:10.1080/09638280500534861

Lagace, D. C. (2012). Does the endogenous neurogenic response alter behavioral recovery following stroke? *Behavioural Brain Research*, *227*(2), 426–32. doi:10.1016/j.bbr.2011.08.045

Lehrmann, E., Christensen, T., Zimmer, J., Diemer, N. H., & Finsen, B. (1997). Microglial and Macrophage Reactions Mark Progressive Changes and Define the Penumbra in the Rat Neocortex and Striatum After Transient Middle Cerebral Artery Occlusion, *476*(February 1996), 461–476.

Lopez-Lopez, C., LeRoith, D., & Torres-Aleman, I. (2004). Insulin-like growth factor I is required for vessel remodeling in the adult brain. *Proceedings of the National Academy of Sciences of the United States of America*, *101*(26), 9833–8. doi:10.1073/pnas.0400337101

MacLellan, C. L., Keough, M. B., Granter-Button, S., Chernenko, G. A., Butt, S., & Corbett, D. (2011). A critical threshold of rehabilitation involving brain-derived neurotrophic factor is required for poststroke recovery. *Neurorehabilitation and Neural Repair*, *25*(8), 740–8. doi:10.1177/1545968311407517

Macrae, I. M., Robinson, M. J., Graham, D. I., Reid, J. L., & McCulloch, J. (1993). Endothelin-1-induced reductions in cerebral blood flow: dose dependency, time course, and neuropathological consequences. *Journal of Cerebral Blood Flow and Metabolism : Official Journal of the International Society of Cerebral Blood Flow and Metabolism*, *13*(2), 276–84. doi:10.1038/jcbfm.1993.34

Min, K.-J., Yang, M., Kim, S.-U., Jou, I., & Joe, E. (2006). Astrocytes induce hemeoxygenase-1 expression in microglia: a feasible mechanism for preventing excessive brain inflammation. *The Journal of Neuroscience : The Official Journal of the Society for Neuroscience*, *26*(6), 1880–7. doi:10.1523/JNEUROSCI.3696-05.2006

Murphy, T. H., & Corbett, D. (2009). Plasticity during stroke recovery: from synapse to behaviour. *Nature Reviews. Neuroscience*, *10*(12), 861–72. doi:10.1038/nrn2735

Neher, J. J., Emmrich, J. V, Fricker, M., Mander, P. K., Théry, C., & Brown, G. C. (2013). Phagocytosis executes delayed neuronal death after focal brain ischemia. *Proceedings of the National Academy of Sciences* , *110* (43), E4098–E4107. doi:10.1073/pnas.1308679110

Ng, Y. S., Stein, J., Ning, M., & Black-Schaffer, R. M. (2007). Comparison of clinical characteristics and functional outcomes of ischemic stroke in different vascular territories. *Stroke; a Journal of Cerebral Circulation*, *38*(8), 2309–14. doi:10.1161/STROKEAHA.106.475483

Nowicka, D., Rogozinska, K., Aleksy, M., Witte, O. W., & Skangiel-Kramska, J. (2008). Spatiotemporal dynamics of astroglial and microglial responses after photothrombotic stroke in the rat brain. *Acta Neurobiologiae Experimentalis*, *68*(2), 155–68. Retrieved from http://www.ncbi.nlm.nih.gov/pubmed/18511952

Ohab, J. J., Fleming, S., Blesch, A., & Carmichael, S. T. (2006). A neurovascular niche for neurogenesis after stroke. *The Journal of Neuroscience : The Official Journal of the Society for Neuroscience*, *26*(50), 13007–16. doi:10.1523/JNEUROSCI.4323-06.2006

Ohta, S., Gregg, C., & Weiss, S. (2006). Pituitary Adenylate Cyclase-Activating Polypeptide Regulates Forebrain Neural Stem Cells and Neurogenesis In Vitro and In Vivo. *Journal of Neuroscience Research*, *84*(August), 1177–1186. doi:10.1002/jnr

Olsen, T. S., & Lassen, N. a. (1984). A dynamic concept of middle cerebral artery occlusion and cerebral infarction in the acute state based on interpreting severe hyperemia as a sign of embolic migration. *Stroke*, *15*(3), 458–468. doi:10.1161/01.STR.15.3.458

Osman, A. M., Porritt, M. J., Nilsson, M., & Kuhn, H. G. (2011). Long-term stimulation of neural progenitor cell migration after cortical ischemia in mice. *Stroke; a Journal of Cerebral Circulation*, *42*(12), 3559–65. doi:10.1161/STROKEAHA.111.627802

Parent, J. M., Vexler, Z. S., Gong, C., Derugin, N., & Ferriero, D. M. (2002). Rat forebrain neurogenesis and striatal neuron replacement after focal stroke. *Annals of Neurology*, *52*(6), 802–13. doi:10.1002/ana.10393

Picanço, M. R., Christensen, S., Campbell, B. C. V, Churilov, L., Parsons, M. W., Desmond, P. M., … Davis, S. M. (2014). Reperfusion after 4.5 hours reduces infarct growth and improves clinical outcomes. *International Journal of Stroke : Official Journal of the International Stroke Society*, *9*(3), 266–9. doi:10.1111/ijs.12209

Ploughman, M., Granter-Button, S., Chernenko, G., Attwood, Z., Tucker, B. A., Mearow, K. M., & Corbett, D. (2007). Exercise intensity influences the temporal profile of growth factors involved in neuronal plasticity following focal ischemia. *Brain Research*, *1150*, 207–16. doi:10.1016/j.brainres.2007.02.065

Price, C. J. S., Wang, D., Menon, D. K., Guadagno, J. V, Cleij, M., Fryer, T., … Warburton, E. a. (2006). Intrinsic activated microglia map to the peri-infarct zone in the subacute phase of ischemic stroke. *Stroke; a Journal of Cerebral Circulation*, *37*(7), 1749–53. doi:10.1161/01.STR.0000226980.95389.0b

Roemer, E., Lammerich, H.-P., Conroy, L. L., & Weisensee, D. (2013). Characterization of a gap-junctional intercellular communication (GJIC) assay using cigarette smoke. *Toxicology Letters*, *219*(3), 248–53. doi:10.1016/j.toxlet.2013.03.028

Roger, V. L., Go, A. S., Lloyd-Jones, D. M., Adams, R. J., Berry, J. D., Brown, T. M., … Wylie-Rosett, J. (2011). Heart disease and stroke statistics--2011 update: a report from the American Heart Association. *Circulation*, *123*(4), e18–e209. doi:10.1161/CIR.0b013e3182009701

Rolls, A., Shechter, R., & Schwartz, M. (2009). The bright side of the glial scar in CNS repair. *Nature Reviews. Neuroscience*, *10*(3), 235–41. doi:10.1038/nrn2591

Roome, R. B., Bartlett, R. F., Jeffers, M., Xiong, J., Corbett, D., & Vanderluit, J. L. (2014). A reproducible Endothelin-1 model of forelimb motor cortex stroke in the mouse. *Journal of Neuroscience Methods*. doi:10.1016/j.jneumeth.2014.05.014

Sabelström, H., Stenudd, M., Réu, P., Dias, D. O., Elfineh, M., Zdunek, S., … Frisén, J. (2013). Resident neural stem cells restrict tissue damage and neuronal loss after spinal cord injury in mice. *Science (New York, N.Y.)*, *342*(6158), 637–40. doi:10.1126/science.1242576

Sairanen, T., Karjalainen-Lindsberg, M.-L., Paetau, A., Ijäs, P., & Lindsberg, P. J. (2006). Apoptosis dominant in the periinfarct area of human ischaemic stroke--a possible target of antiapoptotic treatments. *Brain : A Journal of Neurology*, *129*(Pt 1), 189–99. doi:10.1093/brain/awh645

Saraste, A., & Pulkki, K. (2000). Morphologic and biochemical hallmarks of apoptosis. *Cardiovascular Research*, *45*(3), 528–537. doi:10.1016/S0008-6363(99)00384-3

Schellinger, P. D., Köhrmann, M., Liu, S., Dillon, W. P., Nogueira, R. G., Shuaib, A., & Liebeskind, D. S. (2013). Favorable vascular profile is an independent predictor of outcome: a post hoc analysis of the safety and efficacy of NeuroFlo Technology in Ischemic Stroke trial. *Stroke; a Journal of Cerebral Circulation*, *44*(6), 1606–8. doi:10.1161/STROKEAHA.111.000709

Slepko, N., & Levi, G. (1996). Progressive activation of adult microglial cells in vitro. *Glia*, *16*(3), 241–46. doi:10.1002/(SICI)1098-1136(199603)16:3<241::AID-GLIA6>3.0.CO;2-4

Smith, S. C. (2011). Reducing the global burden of ischemic heart disease and stroke: a challenge for the cardiovascular community and the United Nations. *Circulation*, *124*(3), 278–9. doi:10.1161/CIRCULATIONAHA.111.040170

Sofroniew, M. V. (2009). Molecular dissection of reactive astrogliosis and glial scar formation. *Trends in Neurosciences*, *32*(12), 638–47. doi:10.1016/j.tins.2009.08.002

Stichel, C. C., & Müller, H. W. (1998). The CNS lesion scar: new vistas on an old regeneration barrier. *Cell and Tissue Research*, *294*(1), 1–9. Retrieved from http://www.ncbi.nlm.nih.gov/pubmed/9724451

Stoll, G. (1998). Inflammation and glial responses in ischemic brain lesions. *Progress in Neurobiology*, *56*(2), 149–171. doi:10.1016/S0301-0082(98)00034-3

Takatsuru, Y., Eto, K., Kaneko, R., Masuda, H., Shimokawa, N., Koibuchi, N., & Nabekura, J. (2013). Critical role of the astrocyte for functional remodeling in contralateral hemisphere of somatosensory cortex after stroke. *The Journal of Neuroscience : The Official Journal of the Society for Neuroscience*, *33*(11), 4683–92. doi:10.1523/JNEUROSCI.2657-12.2013

Taylor, R. A., & Sansing, L. H. (2013). Microglial responses after ischemic stroke and intracerebral hemorrhage. *Clinical & Developmental Immunology*, *2013*, 746068. doi:10.1155/2013/746068

Tennant, K. A., & Brown, C. E. (2013). Diabetes augments in vivo microvascular blood flow dynamics after stroke. *The Journal of Neuroscience : The Official Journal of the Society for Neuroscience*, *33*(49), 19194–204. doi:10.1523/JNEUROSCI.3513-13.2013

Teramoto, T., Qiu, J., Plumier, J. C., & Moskowitz, M. a. (2003). EGF amplifies the replacement of parvalbumin-expressing striatal interneurons after ischemia. *Journal of Clinical Investigation*, *111*(8), 1125–1132. doi:10.1172/JCI200317170

Thored, P., Arvidsson, A., Cacci, E., Ahlenius, H., Kallur, T., Darsalia, V., … Lindvall, O. (2006). Persistent production of neurons from adult brain stem cells during recovery after stroke. *Stem Cells (Dayton, Ohio)*, *24*(3), 739–47. doi:10.1634/stemcells.2005-0281

Tsai, P. T., Ohab, J. J., Kertesz, N., Groszer, M., Matter, C., Gao, J., … Carmichael, S. T. (2006). A critical role of erythropoietin receptor in neurogenesis and post-stroke recovery. *The Journal of Neuroscience : The Official Journal of the Society for Neuroscience*, *26*(4), 1269–74. doi:10.1523/JNEUROSCI.4480-05.2006

Tsenov, G., Mátéffyová, A., Mareš, P., Otáhal, J., & Kubová, H. (2007). Intrahippocampal injection of endothelin-1: A new model of ischemia-induced seizures in immature rats. *Epilepsia*, *48*(SUPPL. 5), 7–13. doi:10.1111/j.1528-1167.2007.01282.x

Türeyen, K., Vemuganti, R., Bowen, K. K., Sailor, K. a., & Dempsey, R. J. (2005). EGF and FGF-2 infusion increases post-ischemic neural progenitor cell proliferation in the adult rat brain. *Neurosurgery*, *57*(6), 1254–1262. doi:10.1227/01.NEU.0000186040.96929.8A

Walberer, M., Rueger, M. a, Simard, M.-L., Emig, B., Jander, S., Fink, G. R., & Schroeter, M. (2010). Dynamics of neuroinflammation in the macrosphere model of arterio-arterial embolic focal ischemia: an approximation to human stroke patterns. *Experimental & Translational Stroke Medicine*, *2*(1), 22. doi:10.1186/2040-7378-2-22

Wartenberg, K. E. (2012). Malignant middle cerebral artery infarction. *Current Opinion in Critical Care*, *18*(2), 152–63. doi:10.1097/MCC.0b013e32835075c5

White, R. E., Yin, F. Q., & Jakeman, L. B. (2008). TGF-alpha increases astrocyte invasion and promotes axonal growth into the lesion following spinal cord injury in mice. *Experimental Neurology*, *214*(1), 10–24. doi:10.1016/j.expneurol.2008.06.012

Wiley, K. E., & Davenport, A. P. (2004). Endothelin receptor pharmacology and function in the mouse: comparison with rat and man. *Journal of Cardiovascular Pharmacology*, *44 Suppl 1*(November), S4–6. Retrieved from http://www.ncbi.nlm.nih.gov/pubmed/15838332

Wittko, I. M., Schänzer, A., Kuzmichev, A., Schneider, F. T., Shibuya, M., Raab, S., & Plate, K. H. (2009). VEGFR-1 regulates adult olfactory bulb neurogenesis and migration of neural progenitors in the rostral migratory stream in vivo. *The Journal of Neuroscience : The Official Journal of the Society for Neuroscience*, *29*(27), 8704–8714. doi:10.1523/JNEUROSCI.5527-08.2009

Yuan, Y.-M., & He, C. (2013). The glial scar in spinal cord injury and repair. *Neuroscience Bulletin*, *29*(4), 421–35. doi:10.1007/s12264-013-1358-3

Zeiler, S. R., Gibson, E. M., Hoesch, R. E., Li, M. Y., Worley, P. F., O'Brien, R. J., & Krakauer, J. W. (2013). Medial premotor cortex shows a reduction in inhibitory markers and mediates recovery in a mouse model of focal stroke. *Stroke; a Journal of Cerebral Circulation*, *44*(2), 483–9. doi:10.1161/STROKEAHA.112.676940

Zhu, W., Cheng, S., Xu, G., Ma, M., Zhou, Z., Liu, D., & Liu, X. (2011). Intranasal nerve growth factor enhances striatal neurogenesis in adult rats with focal cerebral ischemia. *Drug Delivery*, *18*(January), 338–343. doi:10.3109/10717544.2011.557785